Working Paper

Impact of Climate Change on Global Sensitivity of Lake Stratification

Gabriela Meyer
Ilya Masliev
László Somlyódy

WP-94-28
April 1994

IIASA International Institute for Applied Systems Analysis □ A-2361 Laxenburg □ Austria
Telephone: +43 2236 715210 □ Telex: 079 137 iiasa a □ Telefax: +43 2236 71313

Impact of Climate Change on Global Sensitivity of Lake Stratification

Gabriela Meyer
Ilya Masliev
László Somlyódy

WP-94-28
April 1994

International Institute for Applied Systems Analysis □ A-2361 Laxenburg □ Austria
Telephone: +43 2236 715210 □ Telex: 079 137 iiasa a □ Telefax: +43 2236 71313

Abstract

Global climate change could significantly influence hydrophysical processes in lakes and reservoirs and affect aquatic ecosystems. The present work addresses possible impacts on thermal household of standing waters. Sensitivity studies were performed to identify the influence of air temperature changes on lake stratification patterns for different geographic zones of the globe. Ice cover and convective overturn events were selected as indicators. Hypothetical waterbodies used in this series of simulations were assumed typical for shallow, deep, and intermediate lakes. A vertical one-dimensional hydrothermal model developed at the Institute for Water and Ecological Problems (Russia) was used to simulate water temperature and components of the thermal energy budget. The model was cross-checked with a similar model WQRRS (University of California-Davis). Simulation results appear to be consistent with existing stratification-based classification of lakes. Sensitivity analysis showed that effect of changing climate is roughly equivalent to a corresponding change in geographic location, approximately one latitude degree per one degree Celsius of air temperature. Zones of higher sensitivity to air temperature change were revealed where changes were especially profound, namely subtropical zone 30^{o}-40^{o} (with respect to cooler climate) and subpolar zone 70^{o}-80^{o} (with respect to warming). Subsequently, nine real lakes were selected from the sensitive regions. Future climate conditions were obtained from the GFDL global circulation model, under an assumption of doubling CO_2 concentration in the atmosphere. For five selected lakes little or no change in monitored indicators was detected, while for four lakes, changes from an existing stratification pattern were found to be significant.

TABLE OF CONTENTS

1. INTRODUCTION

Increased concentrations of greenhouse gases in the atmosphere are considered to result in likely global warming of the lower atmosphere (see e.g. Bolin et al., 1986). A changed climate could significantly affect the hydrologic regime and its various elements. For instance, surface runoff and water availability could be altered leading to serious water management problems. The literature incorporates quite a number of publications on the above issues (Waggoner 1990, Kaczmarek and Krasuski 1991, Nash and Gleick 1991, IPCC 1992, Kundzewicz and Somlyódy 1993). It is evident that our knowledge is becoming increasingly uncertain as we move from the observed changes in concentrations of CO_2 and other greenhouse gases through climate change to possible alterations of hydrology and water management (see Fiering and Matalas, 1990).

The situation is, however, even worse if we consider water quality of surface waters and the impact on aquatic ecosystems. Here we have no more than speculations (see Jacoby, 1990) and a systematic framework was prepared only recently which outline major processes and their interactions affecting water quality (see Varis and Somlyódy, 1993). As examples we note the oxygen household of rivers influenced by the possible change of runoff and oxygen saturation level; the carbon cycle of lakes depending on the partial pressure of CO_2 and temperature (Szilágyi and Somlyódy, 1991); nutrient cycling depending strongly on temperature and its seasonal variations, and on stratification patterns. Studies from the Shasta-Trinity river-reservoir system in California (Orlob et al, 1990) also show that in reservoirs epilimnion temperatures as well as epilimnion depth throughout the year are very sensitive to changes in atmospheric conditions. The study also demonstrates that fishery may be severely affected by water temperature changes. It is evident from the above list that water temperature is a crucial indicator from the viewpoint of the impact of climate change. It is a physical parameter characterizing water quality directly, also having an indirect impact through a number of processes, particularly if we consider lakes and reservoirs.

The question of how freshwater lake temperatures respond to changed atmospheric conditions was addressed recently by Hondzo and Stefan (1991). Three dimictic lakes located near 45^{o} N latitude and 93^{o} W longitude in the north central United States were selected. Historical records were used to specify a "warm (future) climate" scenario (the summer of 1988) and a "normal" (past) condition (the year 1971). A vertically one-dimensional hydrothermal model was used to analyze spatial and temporal changes in temperature, as well as in components of the thermal energy budget and in the stratification pattern. The study indicated a high sensitivity in epilimnetic water temperature and an increase in surface mixed layer depths.

The present paper will address the same question. However the context, and thus the approach, will be quite different. Instead of a detailed analysis of a small number of specific lakes, our primary aim is to raise a broader question, i. e., what is the regional sensitivity of lake stratification patterns to future climate change depending on latitude and longitude? A possibility to study this issue would be to evaluate past and future thermal behavior for a large number of lakes of various morphologies and locations by a proper heat budget model. However, such an approach is not practical as the data and labor requirement would be tremendous.

For this reason we decided to follow a three-step procedure. The first step incorporates the definition and analysis of a number of hypothetical lakes (from shallow to deep) to identify sensitive regions of the globe by changing systematically the location (in terms of latitude). In the second step real lakes are selected from the sensitive regions defined in step 1, still maintaining a number of simplifying assumptions related to morphology, inflow and outflow, etc. (see below). Base case simulations use monthly averaged historical climatic data while future conditions are obtained from a global circulation model (GCM). Both scenarios depend on latitude and longitude. The third stage is beyond the scope of our present effort: it is the detailed analysis of the same set of lakes as in the second step by using specific data and resolving the simplifying assumptions.

The paper is organized as follows. First we offer a detailed problem formulation followed by an outline of the approach to be employed (Chapters 2 and 3). Chapter 4 summarizes properties of data bases to be used for generating historical and future climatic scenarios. Chapter 5 discusses major features of thermal models which will serve as basic tools for our study. A simplified method is outlined here which is then used for the specification of hypothetical lakes (Chapter 6). The identification of sensitive regions and the selection of real lakes are the subject of Chapter 7. Results obtained and their discussion is given in Chapter 8.

2. PROBLEM FORMULATION

The heat balance in a lake is a result of heat absorption, dissipation and distribution within the entire water body. Heat absorption takes place at the surface of the water. The low thermal conductivity of water prevents heat redistribution into deeper layers, which is possible almost entirely due to mechanical energy, wind being the most important driving force. It is therefore expected that any changes in meteorologic and climatic conditions can affect the thermal household of the system.

The surface heat transfer of a lake depends on several components such as net short wave (solar) radiation, net long wave (atmospheric) radiation, water surface back radiation, evaporative loss and conductive loss (see e.g. Orlob, 1983; Octavio et al., 1977). Net solar radiation depends on the clear sky solar radiation, a function of latitude and time of the year, and cloudiness. Net long wave radiation basically hinges upon air temperature (cloudiness and air humidity also plays a role), while water surface back radiation is determined by the surface water temperature. The evaporative heat flux is a function of the water pressure (or specific humidity), wind speed, and surface water temperature. In addition to these, the conductive loss is also influenced by the air temperature.

The above brief review shows that a change in climate would affect the heat balance of lakes primarily by factors such as air temperature, cloudiness, relative humidity, and wind speed. Among these, air temperature is very important. Its potential increase results in higher atmospheric radiation and modifications in backwater radiation, evaporation losses, and heat conduction. The likely end result of all these changes is an increase in the surface water temperature. We note that for the lakes studied by Hondzo and Stefan (1991) the average air temperature of the period May-August was approximately 3^{o} C higher in 1988 than in 1971, leading to a similar increase in the average epilimnion temperature (the difference between 1977 and 1988 conditions fluctuated between -4^{o} C and $+ 10^{o}$ C, with approximately only two months with negative differences, i.e. colder conditions in the future scenario). The

changes in hypolimnetic temperatures were much smaller and somewhat inconsistent. It was found, by comparison of simulations for the "warm" and "normal" summers, that higher back radiation (due to higher epilimnion temperatures) compensated for the increase in atmospheric radiation. Conductive heat transfer turned out to have a negligible effect, while evaporative heat loss increased by about 40%.

The heat balance of a lake obviously depends on transformation processes in the water body. Deep lakes and reservoirs are subject to a phenomenon called stratification. Stratification occurs due to heat flux differential along the depth resulting in the formation of a stable density profile with denser water layers below lighter ones (Wetzel, 1983). Lakes and reservoirs experience seasonal changes in their degree of stratification (see e.g. Octavio, et al. 1977). The characteristic degree of stratification depends on climatic factors as well as morphology, and in the case of reservoirs the through flows. In temperate zones, in early spring a lake is isothermal with typical temperatures at about 4 ^{o}C. As the season progresses the lake begins to warm and differential absorption of heat induces stratification forming the epilimnion and hypolimnion. Later during cooling periods if the surface temperature drops below the temperature of the water beneath, convective mixing occurs through density instabilities due to the formation of denser water at the surface. Pronounced water circulation and mixing eventually can destroy thermal stratification and water turnovers are manifested, particularly when surface waters reach 4 ^{o}C, i.e. maximum water density. Overall wind mixing contributes to maintain a mixed upper layer, a situation especially enhanced when the water temperatures are low due to the lower density gradients in the cold water ranges.

An alteration of the magnitude and timing of the climatological factors that drive stratification can thus change the stratification pattern and possibly also the overturns that strongly influence water quality and the behavior of aquatic ecosystems. Under stratified conditions, the deeper water is isolated from the atmosphere impeding oxygenation of such layers. Further, decomposition of organic matter in the bottom may deplete oxygen and create anoxic conditions that foster the growth of anaerobic microorganisms. Lakes with overturn periods temporarily experience a mixing of the whole water column. It is evident that if there is a significant change in the length of the stratified period and number of overturns, material cycling can be drastically altered. Under extreme conditions, it may not be excluded that deep lakes can behave like shallow ones or vice versa.

The objective of the present paper is to study whether such changes can occur and if so, in what regions of the world. An interrelated question is at what extent would duration of stratified and ice cover periods change? In other words, our interest is to evaluate the regional sensitivity of lakes to the impact of climate change on stratification.

The above issue is closely related to geographical classification used in limnology (see e.g. Wetzel, 1983). The thermal behavior of lakes changes with latitude and altitude locations depending on the relation of the seasonally variable water temperature and the point of maximum density (4 ^{o}C). Accordingly six distinctive categories can be identified as follows:

i) Amictic polar lakes of permanent ice cover;

ii) Cold monomictic lakes in the latitude range of 60^{o} - 80^{o} which circulate fully during summer;

iii) Dimictic (temperate) lakes in the latitude range of 40^{o} to 60^{o}, having two turnovers in a year (most of the North Euro-Asian and North American lakes belong to this group);

iv) Warm monomictic lakes of subtropical type (20^{o} - 40^{o}) which show circulation only during the winter;

v) Oligomictic lakes, of no or rare circulation, are located close to the equator at low latitudes;

vi) Polymictic water bodies in latitude domains close to the equator, with frequent turnovers due to high altitudes and intense cooling at night.

Another type of obvious distinction exists between shallow lakes and deep ones. For shallow lakes the depth is not sufficient for a hypolimnion to form and stratification can only be maintained temporarily. The mixing depths of lakes depend primarily on the wind speed. According to Schwoerbel (1987), 1-2 m mixing depth corresponds to 2 m/s wind speed, while 6-12 m correspond to 10 m/s. The depth required to become thermally stratified varies greatly with site specific features such as surface area, the volume to depth relation, the prevailing wind direction, the fetch, the protection by surrounding topography and vegetation, and others.

The geographical classification depends also on morphology and other local conditions. A dimictic or monomictic lake should be deep enough to have the hypolimnion developed (in contrast, a shallow lake can be considered as polymictic). We note the role of altitude: the behavior of standing waters located at higher altitudes is similar to that of lower ones but in higher (colder) latitudes. Low latitudes lead to exceptions in the above categories, primarily due to the strong influence of oceanic climate (Wetzel, 1983).

Having the two interrelated classification systems defined (geographical and geomorphological), we may be interested to know whether a shift in classes along the latitude will not be the result if a climate change takes place. Similarly, we may study whether, depending on location, a switch of a lake from deep to shallow is possible which would then have serious implications from the viewpoint of material cycling and water quality as noted earlier.

3. APPROACH

The regional analysis of climate change on lakes and the approach adopted directly stem from the formulation of objectives. It is envisioned as follows.

First climate data from data bases are retrieved in order to formulate realistic systematic analysis. The available data are: 1) longitudinally averaged historic data set; 2) long-term monthly average data for a large number of stations (of different latitudes and longitudes); 3) predictions of future changed climate from Global Circulation Models (GCMs) (for details see Chapter 4).

Next, two hydrodynamic models are compared in order to select the most appropriate one for the analysis. These models are: 1) the model developed by the Institute for Water and Environmental Problems (IWEP), Siberian Branch of the Russian Academy of Sciences, in Barnaul, Russia; and 2) the hydrothermal component of the Water Quality of River and Reservoir Systems model (WQRRS) developed for the US Army Corps of Engineers. As will be seen in Chapter 5, the similarity of the simulations performed by the two models leads to

the use of the IWEP model because the running time is shorter and it is capable of simulating overturn periods and ice cover.

To produce systematic runs whereby the behavior of shallow to deep water bodies are assessed, hypothetical lakes are generated, all of them having surface area of 100 km^2 and parabolic bathimetry. The selection of the depth of shallow, medium, and deep lakes is performed using a simplified two-layer version of the MIT wind-mixing model (Octavio, et al., 1977). It is computationally efficient and well-suited for the purpose (see Chapter 6).

Next, latitudes where lakes are sensitive to air temperature change are identified using the IWEP model, hypothetical lakes, and the historic longitudinally averaged monthly data.

Real water bodies (lakes and reservoirs) were then chosen within the identified sensitive latitude fringes. The morphology of these lakes is characterized in a simplistic fashion on the basis of real surface area pertaining to real mean depth.

Present climate scenarios are formulated using real station monthly averaged climatic data (for each water body the closest station is used). Future scenarios in which a doubling of atmospheric CO_2 is assumed, are derived from the Global Circulation Model of the Geophysical Fluid Dynamic Laboratory (GFDL) of NOAA.

4. DATA USED

As outlined earlier, three main sets of meteorological data were needed. One of them contains monthly longitudinally averaged historic data which was used to test overturn sensitivities at different latitudes. A second set contains historic observations at weather stations belonging to various latitudes and longitudes. This data set was applied to produce present (base) case scenarios. The third data set is the GFDL GCM output, used to derive global climate change (future) scenarios. A detailed description of these data sets follows.

4.1 Longitudinally and Monthly Averaged Data

Longitudinally averaged monthly climate data were obtained from the report of Telegadas and London, 1954, which compiles 30 years of data recorded prior to 1954, and includes temperature, relative humidity, wind speed, cloudiness, and pressure. The observations were first averaged for summer and winter conditions and then longitudinally, i.e. all station data within a 10^o latitude range were averaged. Since the procedure of averaging is not straightforward and requires accurate processing, this set was used for simulation rather than similarly processed station data from IIASA dataset. Moreover, the climate data series is longer in the Telegadas and London set. Data were further converted to monthly values by interpolation. Sinusoidal interpolation was used for temperature, relative humidity, and cloudiness; quadratic interpolation was applied for wind speed; no interpolation of pressure data was necessary. Latitudinal changes of major parameters are illustrated in Figures 4.1 to 4.5.

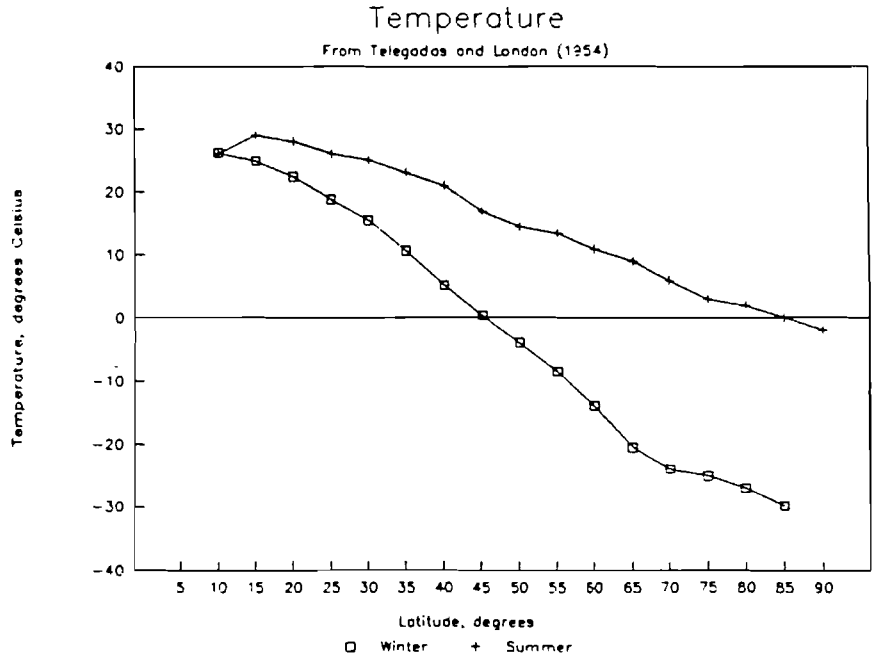

Figure 4.1 Historic longitudinally averaged temperature.

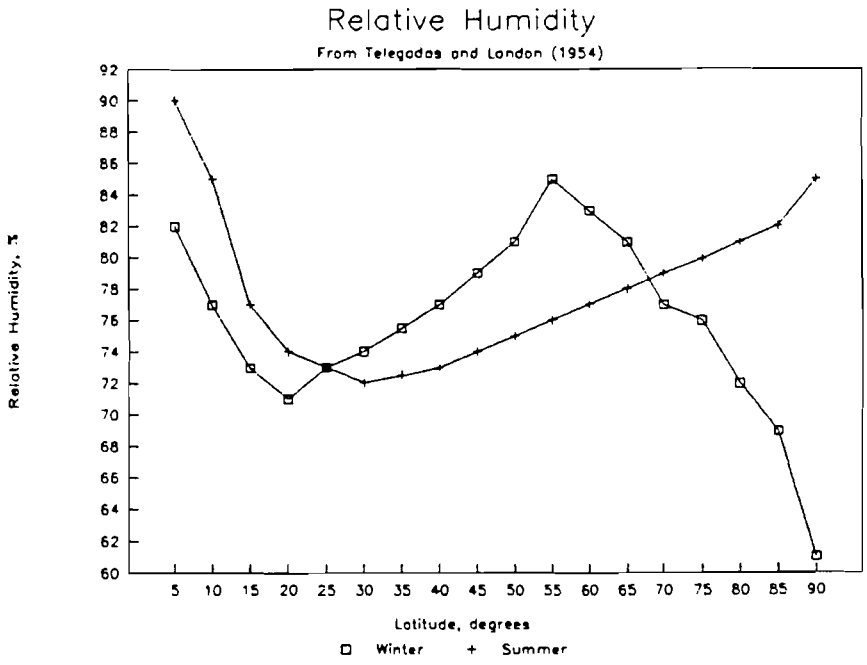

Figure 4.2 Historic longitudinally averaged relative humidity.

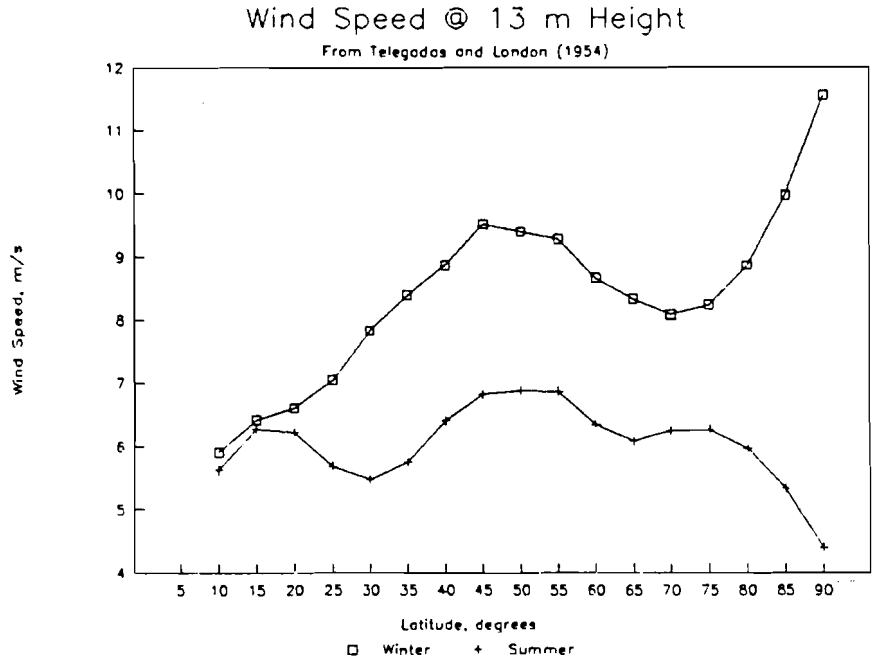

Figure 4.3 Historic longitudinally averaged wind speed.

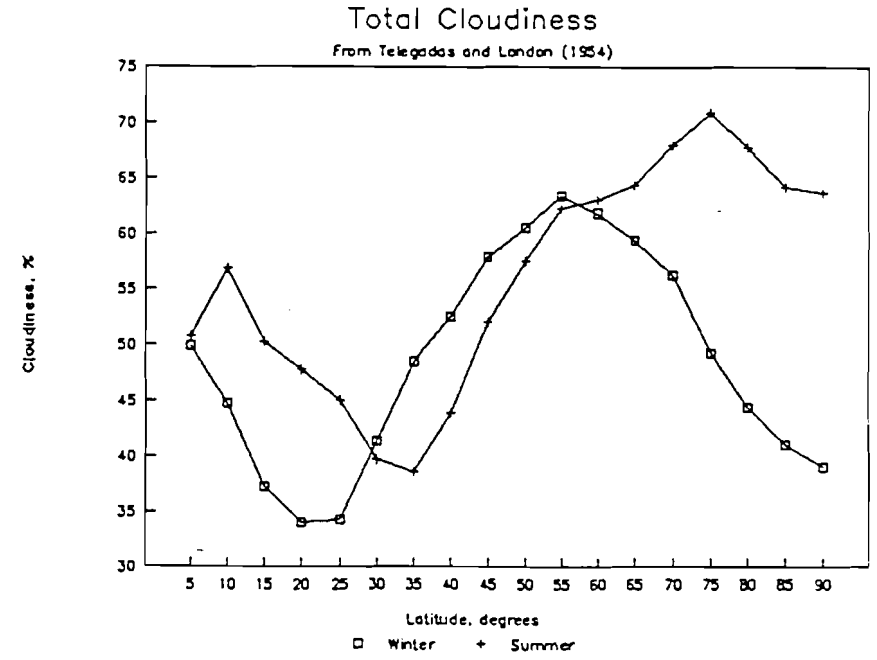

Figure 4.4 Historic longitudinally averaged cloudiness.

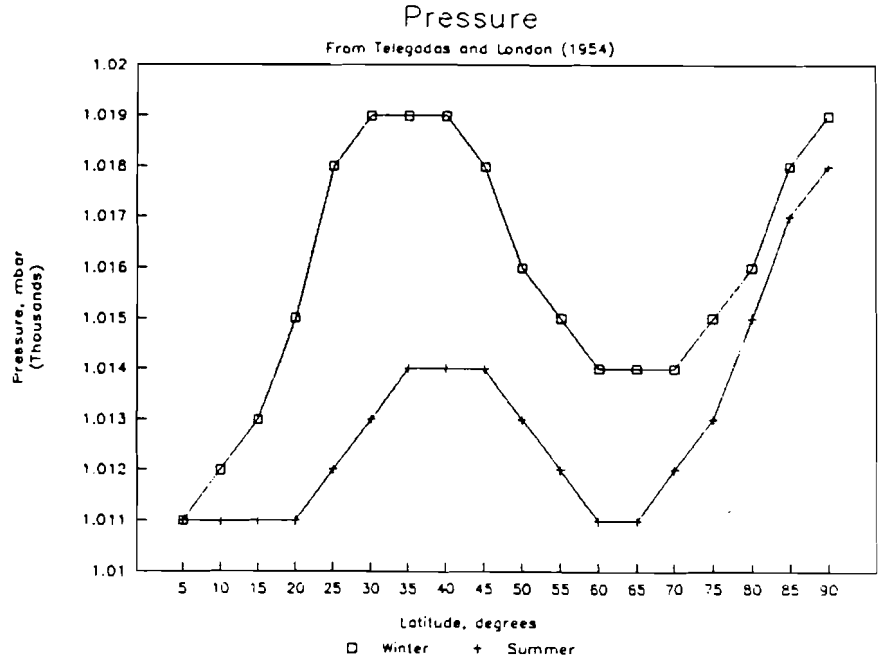

Figure 4.5 Historic longitudinally averaged pressure.

4.2 Historical Observations

Historical observations of climate stations were obtained from the database of IIASA developed by Leemans and Cramer (1991). This database is a compilation of the following weather records:

1. World Weather Records, 1940-1951, (Weather Bureau, 1959).
2. Klimadiagram-Weltatlas, (Walter and Lieth, 1960-1967).
3. Selected Global Climatic Data Set for the Vegetation Science (Müller, 1982).
4. Selected Climate Tables for the World, (UK Meteorological Office, 1966, 1972, 1973, 1978, 1980, 1983).

Leemans and Cramer integrated all these records into a single database within one format, which covers the following variables: mean daily temperature, mean daily maximum temperature (average of daily maximums along the historic records), mean daily minimum temperature (average of daily minimums along the historic records), absolute maximum temperature, absolute minimum temperature, mean relative humidity, mean precipitation, maximum precipitation, minimum precipitation, maximum precipitation in 24 hours, mean number of days with precipitation > 2.5 mm, mean duration of sunshine, mean quantity of radiation, mean potential evapotranspiration, mean wind speed, mean predominant direction of the wind in degrees, soil moisture and monthly total transmittance.

These records are monthly averages over the period of 1941-1960 (some stations have data for a shorter time period within the same period). This period was chosen by Leemans and Cramer as being representative of what they defined "current climate". All the station data

were separately checked for coding errors by evaluating extreme values and averages, and by comparing each station with other stations in the immediate surroundings. The longitude and latitude for each station (location) were also checked.

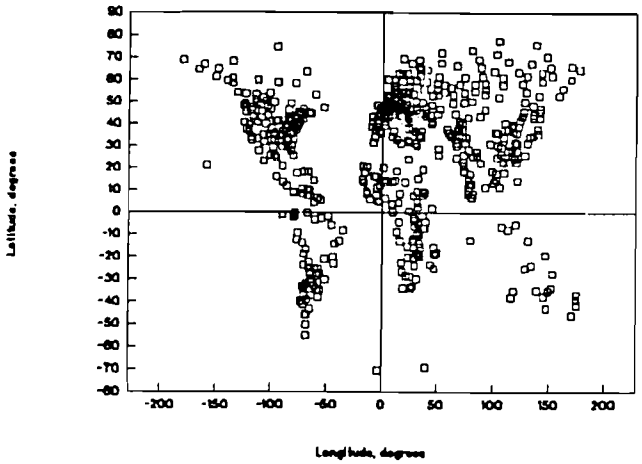

Figure 4.6 Selected climate monitoring stations (For details see Leemans and Cramer (1991))

Unfortunately, data on cloud cover were lost from the database. To resolve this problem the interpolated cloudiness data from Leemans and Cramer (1991) were used (interpolated to a 0.5^{o} latitude x 0.5^{o} longitude grid). Implementation of the original station data with cloudiness was done using the value of the grid point nearest to each of the stations. It was decided that this method was sufficiently accurate given the small distances among grid points.

A subset of stations was then selected. The selection was based on choosing only those stations that would have the following variables:

1. mean daily temperature
2. mean relative humidity
3. mean wind speed
4. mean predominant direction of the wind
5. cloudiness

Figure 4.6 shows the location of this subset of stations. A total of 540 stations were available.

4.3 GCM Data

Global Circulation Model data from the IIASA database were also obtained. It was decided to use the simulation results of the Geophysical Fluid Dynamic Laboratory (GFDL) of NOAA (Manabe, Stoufffer, 1980), because a comparative analysis showed that this model predicts existing conditions on the average more accurately than other GCMs. According to the

analysis done by Kalkstein (1991), GFDL predictions differ from existing conditions only by at most 3 ^{o}C in North America, Europe and Western Euro Asia. In Tropical Asia, Australia, Africa and South America the GFDL predictions reveal colder temperatures than existing conditions, although its predictions are better than those forecasted by the Goddard Institute for Space Studies Model (GISS), and worse than the other GCMs, without these yielding a good representation.

The variables obtained from the GFDL model include monthly mean precipitation and temperature. Both variables are given for present conditions ($1XCO_2$) and a future one assuming a doubling of CO_2 ($2XCO_2$). The variable used for the analysis was the temperature for both scenarios because it is the most important one from a hydrophysical point of view (and it is available from our database).

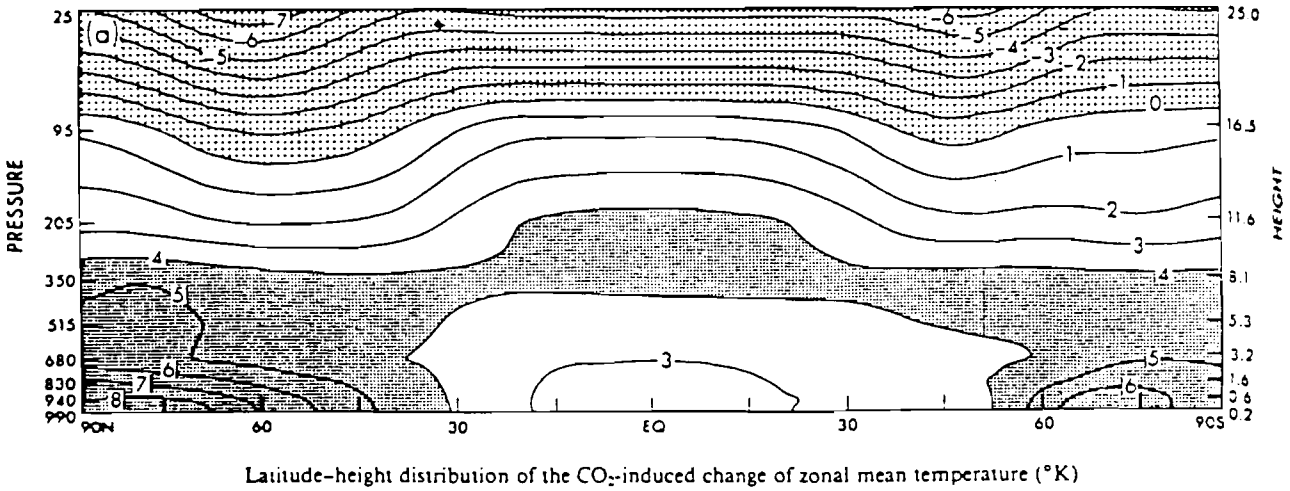

Figure 4.7 GFDL longitudinally averaged predictions on air temperature differences (Source: Wetherald and Manabe [1988]).

GCM output analysis reveals that given the relatively coarse of the GCMs (4^{o} latitude X 5^{o} longitude or ca. 500 x 500 km for the GFDL model) within the boundary layer (2 to 3 km height) temperature difference tendencies are rather homogeneous (Harrison, 1990). For this reason, in order to predict future scenarios the difference in temperature was calculated without requiring altitude adjustments to the GCM temperature data. The future scenarios of air temperature were assessed by adding the GCM temperature difference obtained from the GCM to the present condition station data. GFDL longitudinally averaged predictions on air temperature differences are shown in Figure 4.7.

5. BRIEF DESCRIPTION OF HYDROTHERMAL MODELS

To study the impact of climate change on the hydrothermal dynamics of lakes, three models were considered. Two of them are well known water quality models: Water Quality of River-Reservoir Systems (WQRRS), based on an US Army Corps of Engineers model (HEC, 1978), and the Institute for Water and Environmental Problems model (IWEP), a model from the Siberian Branch of the Russian Academy of Sciences (Zinoviev et al., 1990). For our purposes, their hydrothermal components were used.

A third model was applied solely for generating hypothetical lakes. As already noted, it is a simplified version of the MIT wind-mixing model (Octavio, et al., 1977; see Appendix).

5.1 Hydrothermal Simulation in the WQRRS and IWEP Models

The WQRRS and IWEP models are vertically one-dimensional models of deep stratified reservoirs, assuming full mixing in horizontal layers. Both models have been successfully applied to simulate hydrothermal and water quality dynamics of reservoirs. Internal transport of heat and mass occurs only in the vertical direction as a result of a material balance among layers, which is described by the advection-diffusion equation of the form

$$V\frac{\partial T}{\partial t} = -\Delta z Q_z \frac{\partial T}{\partial z} + \Delta z\, A_z D_c \frac{\partial^2 T}{\partial z^2} + Q_i T_i - Q_o T \pm V \frac{H}{\rho_w c_p}, \qquad (1)$$

where:

T	=	water temperature;
V	=	volume of the fluid element;
t	=	time coordinate;
z	=	space coordinate;
Q_z	=	vertical advection;
A_z	=	element surface area normal to the direction of flow;
D_c	=	effective diffusion coefficient;
Q_i	=	lateral inflow;
T_i	=	inflow thermal energy or constituent concentration;
Q_o	=	lateral outflow;
H	=	internal distribution of heat source within the water column;
C_p	=	heat capacity of water under constant pressure;
ρ_w	=	water density.

5.2 Similarities Between the Two Models

5.2.1 Heat Source

At the water surface the heat source, H, is the result of heat exchange at the air-water interface. The rate of heat transfer per unit of surface area is a the net balance among incoming heat from short and long wave radiation, losses from water surface back radiation, evaporation losses and convection losses/gains. The heat balance equation takes then form

$$H = H_{sn} + H_a + H_w + H_e + H_c, \qquad (2)$$

where:

H_{sn}	=	short wave (solar) radiation;
H_a	=	long wave (atmospheric) radiation;
H_w	=	back water radiation
H_e	=	evaporative loss;
H_c	=	conductive loss/gain.

Short wave radiation in the models is represented as

$$H_s = H_o f(a)(1 - 0.65C^2)(1 - r), \quad (3)$$

where:

H_o = incoming solar radiation at the top of the atmosphere, dependent on the latitude, time of the year, and hour of day;

f(a) = atmospheric transmission term, a function that computes the amount of heat scattered and absorbed by the atmosphere;

C = cloudiness coefficient;

r = albedo or reflection coefficient of the water body's surface.

The amount of short wave radiation that penetrates beyond the surface layer is calculated as a function of the light attenuation capacity of the water body according to the Beer-Lambert law (essentially an exponential decay).

Atmospheric radiation is represented by the Stefan-Boltzman equation:

$$H_a = \sigma \varepsilon T_a^4, \quad (4)$$

where:

σ = Stephan-Boltzman constant;

ε = atmospheric emissivity, function of cloudiness typically expressed as: $\varepsilon = f(1 + 0.17\, C^2)$;

T_a = air temperature.

It is noted that WQRRS uses a finer representation for H_a, whereby the air temperature is raised to the sixth power and the coefficients are readjusted. This fit to atmospheric radiation has been found to be more accurate (TVA, 1972), and it is an adjustment to the fact that the atmosphere is not a black body as expressed with the Stefan-Boltzman equation corrected for a grey body through the emissivity coefficient.

Evaporative losses are calculated in both models with a Lake Hefner type equation of the form

$$H_e = k(a + bW)(e_s - e_a), \quad (5)$$

where:

k = empirical evaporation coefficient which also involves latent heat of vaporization and water density;

a,b = empirical evaporation coefficients;

W = wind speed;

e_s = saturation vapor pressure;

e_a = atmospheric vapor pressure.

It is important to note that calibration studies have shown that the evaporation constants, a and b, have been found to be very sensitive, reflecting their influence in the surface water temperatures.

Losses due to conduction are calculated as

$$H_c = \rho_w c_p f(W)(T_a - T_s), \quad (6)$$

where:

f(W)	=	wind-dependent function;
T_S	=	temperature of the water surface;
T_a	=	atmospheric temperature.

5.2.2 Allocation of Inflow

Inflow allocation in both models is based on the assumption that the inflow water will seek a level of equal density within the lake. If the inflow water density is outside the range of densities found within the lake, the inflow is deposited at either the surface (if the inflow density is lower than that of the surface layer), or at the bottom (if the inflow has a higher density than that of the bottom layer).

Once the entry level is established allocation of inflow to individual elements proceeds using the Debler-Craya criterion (HEC, 1978).

5.3 Differences Between the Models

5.3.1 Diffusion Coefficient

The main difference between the two models stems from the formulation of the diffusion coefficient (representing both molecular and turbulent diffusion mechanisms).

In the case of WQRRS the user can select two methods to calculate effective diffusion: the stability method and the wind method.

i. Stability Method: This procedure is appropriate for most deep and well stratified lakes, or lakes where wind is not the dominant turbulent mixing force. It is based on the assumption that mixing will be at minimum when the density gradient or water column stability is at maximum. The user can choose from a range of effective diffusion coefficients reported in the manual, which were experimentally obtained. Two effective diffusion coefficients are defined: one for the epilimnion and hypolimnion, and a second one for the metalimnion.

ii. Wind Method: It is assumed that wind induced mixing is greater at the surface and diminishes exponentially with depth. The method uses an empirical exponential equation as a function of wind speed and depth to the thermocline ratio.

In the IWEP model the turbulent portion of the effective diffusion coefficient, D_C, is calculated as a function of turbulent kinetic energy and dissipation rate:

$$D_c = c_4 \frac{e^2}{\varepsilon}, \quad (7)$$

where:

c_4	=	constant assumed to be equal to 0.09;
e	=	turbulent kinetic energy;
ε	=	dissipation rate of turbulent energy.

To compute this coefficient a detailed turbulent submodel is used, which includes state variables as follows: w, the vertical velocity component; and u and v which are horizontal velocity components as well as e and ε. Governing equations for each state variable are similar to the transport equation for the temperature (see Equation (1)). Turbulence generation parameters are "confined" in the water volume and are not subject to import/export processes such as vertical or horizontal transport as in other turbulence models. Source terms in the equation of turbulent energy describe energy generation due to velocity shear and turbulent energy generation/suppression in the presence of density stratification. Sink terms describe dissipation of turbulent vorticity by means of transport of large scale motion to a lesser scale and subsequent dissipation of the latter on the molecular viscosity scale. Therefore the following equation holds for turbulent energy:

$$\frac{\partial}{\partial t}(A_z e) = \frac{\partial}{\partial z}(A_z D_c \frac{\partial e}{\partial z}) + c_1 c_4 \frac{e^3}{\varepsilon^2}((\frac{\partial u}{\partial z})^2 + (\frac{\partial v}{\partial z})^2 - (1 - c_3) g \alpha_t \frac{d\rho}{\rho_0 dz}) - \varepsilon, \qquad (8)$$

where:

c_1, c_3	=	model constants;
α_t	=	water volumetric temperature coefficient;
g	=	gravity acceleration, and
ρ	=	water density.

The term including the vertical gradient of water density represents stratification feedback to the diffusion processes. If the density gradient is positive (e.g. an unstable density distribution), an increase in turbulent energy is caused which in turn results in greater turbulent diffusivity D_C. Subsequent intensification of diffusion processes leads to homogenization of temperature and density profiles of (overturn situation). Thus, in this model the sign of the density gradient can be used as an indicator of the initialization of overturn.

5.3.2 Ice Cover and Overturns

The other source of differences is the fact that WQRRS is not implemented to simulate situations where an ice cover forms on the surface, or in general when overturns occur.

In the IWEP model, the ice cover submodel starts its operation when temperature of the upper boundary reaches zero degrees and the boundary condition is adjusted accordingly. In this case heat balance is determined in accordance to the air-ice interface boundary. Ice is assumed to be homogeneous. Temperature distribution in this version of the ice submodel is assumed to be linear, although there is a version of the program code that can account for a nonlinear temperature profile of ice. The time derivative of ice thickness is based on the heat balance of the lower boundary where ice is in contact with water, i. e. at the point where ice is at melting temperature. When the ice thickness is decreased below certain predefined value (stability

level), ice cover is assumed to be destroyed and the boundary condition for water temperature at the upper boundary is switched back to open surface state.

5.3.3 Allocation of Outflow

The IWEP model uses the method proposed by Markofsky and Harleman (1971) and assumes a Gaussian outflow profile.

The WQRRS model offers two options for the determination of outflow location:

i. Debler-Craya withdrawal allocation method, which computes the thickness of the flow field about the center line of the outflow as a direct function of withdrawal rate, density and inverse function of effective width and density gradient at the withdrawal allocation. The outflows are withdrawn assuming uniform velocity distributions within the flow field.

ii. The WES withdrawal allocation method assumes the velocity of the outflow as being directly proportional to the density gradient and to the vertical distance from the elevation center line of the orifice to the upper limit of the zone of withdrawal, and inversely proportional to the density at the outflow and to the area of the orifice. Non uniform outflow velocity distributions can be computed with this method.

5.4 Simulations for Comparing the Two Models

The WQRRS and IWEP models were compared using the set of input data developed for the simulating the Shasta Reservoir in California. The WQRRS model has been calibrated and used for climate change studies for this reservoir (Meyer and Orlob, 1992). The IWEP model was then calibrated on the basis of the simulated temperature profiles of the WQRRS monthly runs. The calibration parameters were equivalent evaporation and diffusion coefficients.

Figures 5.1 to 5.6 show the comparison profiles for every other month of the year. Each profile presented is the result of the simulation on the 15th day of each month, assuming that this profile is representative of the whole month. From the figures it is evident that earlier in the year, i.e. January through July both models yield similar profiles. This situation can be partly explained by the influence of the initial isothermal conditions, common in both models and specified at the beginning of the year. The calibration showed a high sensitivity in terms of the evaporation coefficients. Proper setting of common evaporation coefficients for the two models yielded similar surface water temperatures for the first eight months of the year. In September, as cooling initiated, the differences between the two models increased. The profile for a typical September condition (Figure 5.5) shows that while WQRRS produces faster mixing within the epilimnion, the IWEP model results in a smoother profile. This can be explained by the fact that WQRRS uses a routine which does not allow a top layer to be denser than a lower one. When cooling events occur, the model calls for immediate convective mixing of the layers resulting in the formation of more uniform profiles in the epilimnion. The diffusion technique used by the IWEP model may yield a smoother distribution of heat and thus smoother temperature profiles.

Overally, the profiles generated by both models agree well. Given the fact that the simulation time of the IWEP model is much shorter than that of WQRRS, and that the IWEP model can simulate ice cover and overturns, the IWEP model was chosen for further computations.

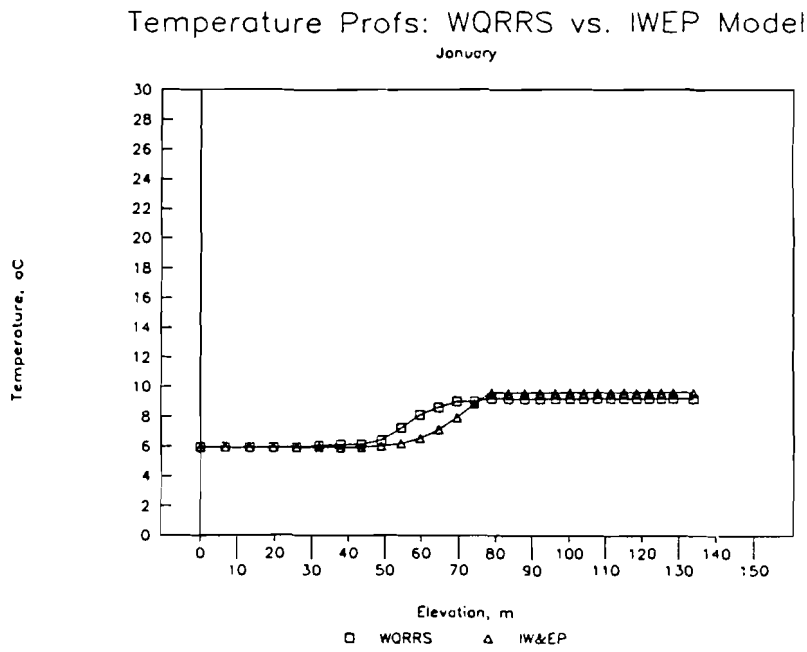

Figure 5.1 Comparison of temperature simulations of the WQRRS and IWEP models: January

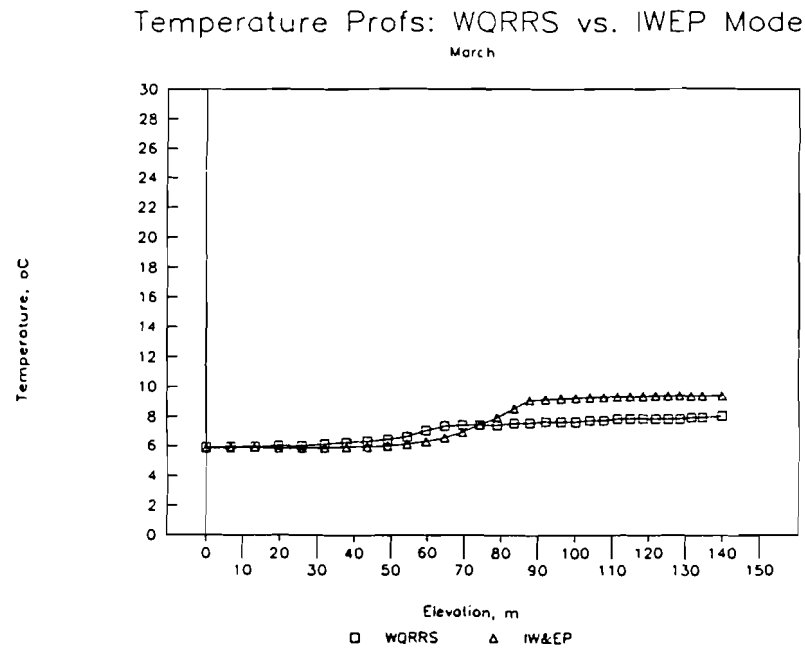

Figure 5.2 Comparison of temperature simulations of the WQRRS and IWEP models: March

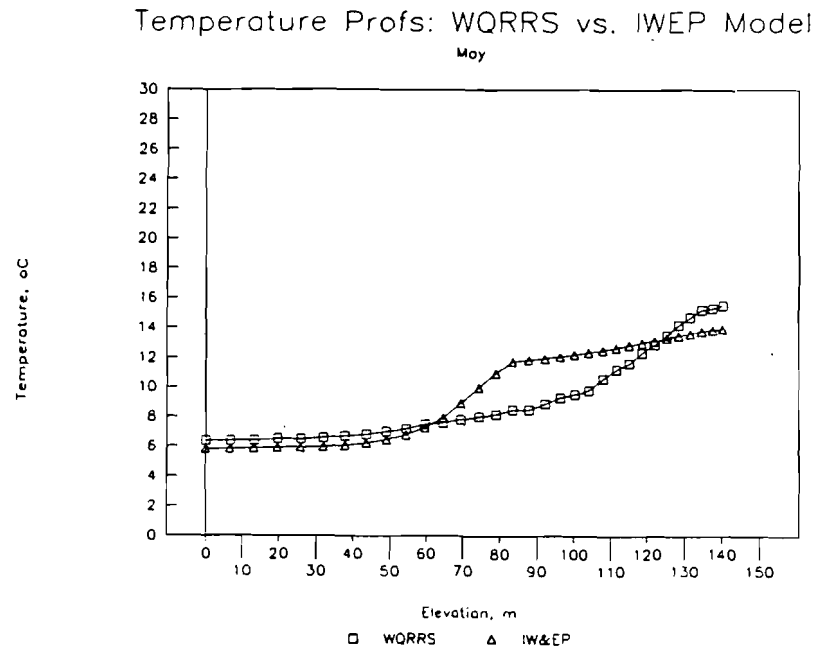

Figure 5.3. Comparison of temperature simulations of the WQRRS and IWEP models: May

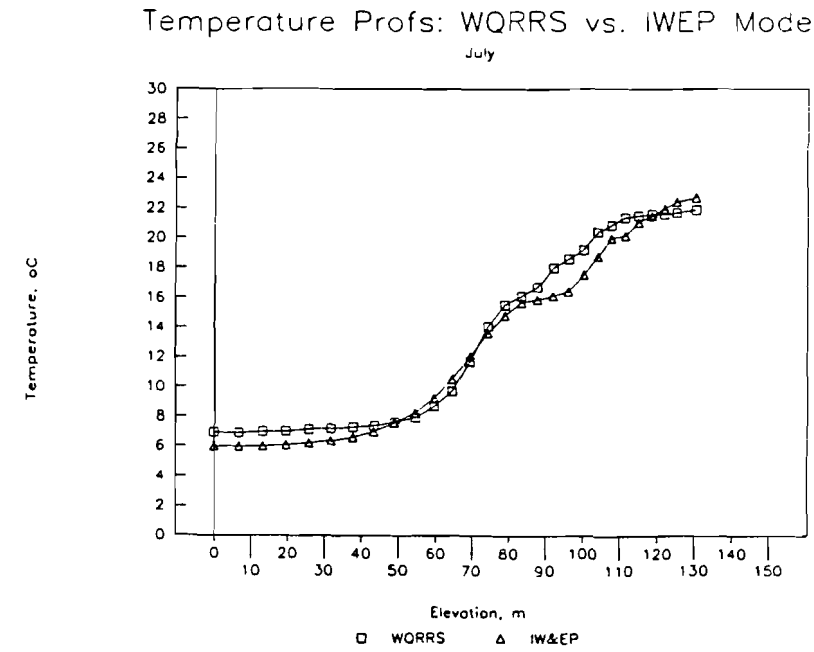

Figure 5.4 Comparison of temperature simulations of the WQRRS and IWEP models: July

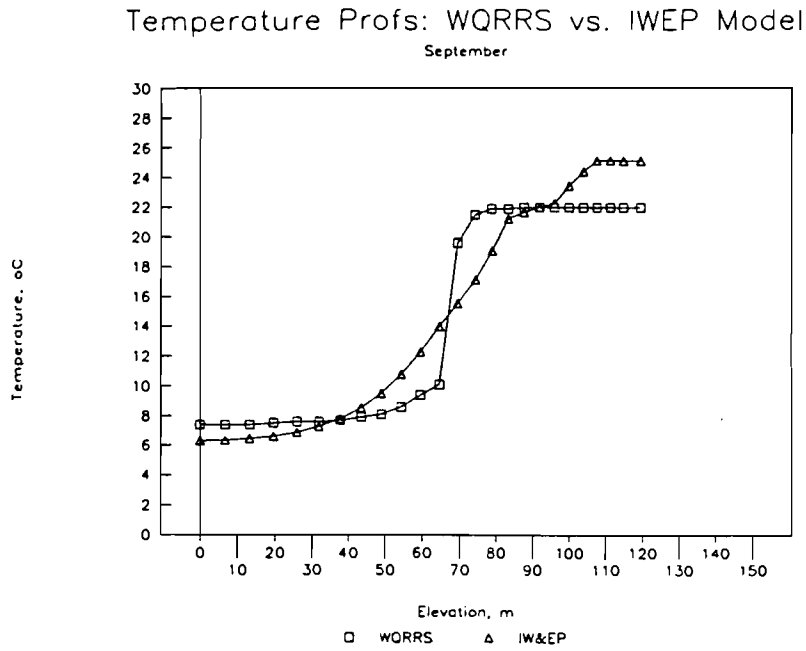

Figure 5.5 Comparison of temperature simulations of the WQRRS and IWEP models: September

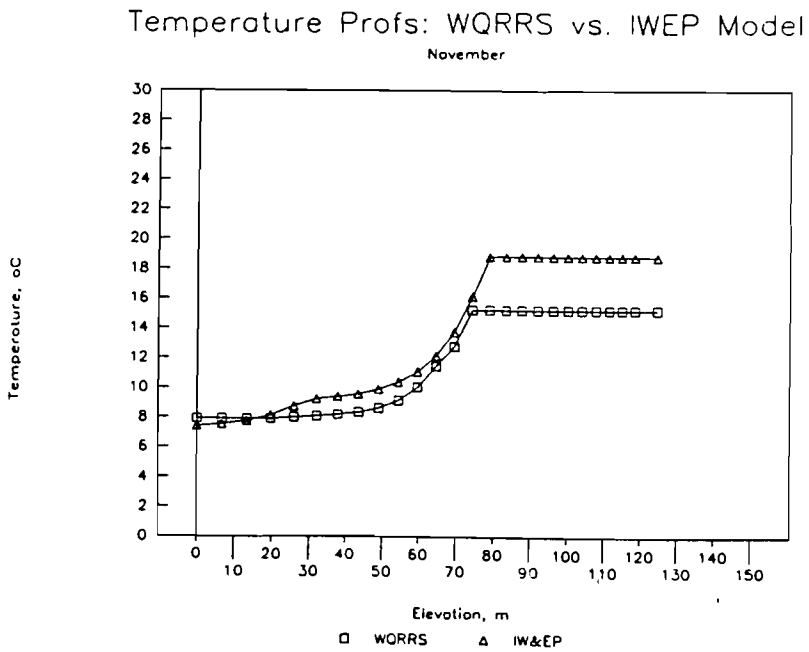

Figure 5.6 Comparison of temperature simulations of the WQRRS and IWEP models: October

6. DETERMINATION OF HYPOTHETICAL LAKES

6.1 Methodology

Thermal characterization of lakes and reservoirs depends on the atmospheric heat influx as well as their hydraulics which in turn depend on morphology. In a reservoir, residence time critically determines its stratification characteristics. Reservoirs with short residence time are frequently mixed water bodies. Others with long residence time can exhibit horizontal stratification. In the case of lakes, negligible inflows and outflows make the thermal household of this system independent of throughflows. To avoid the problem posed by throughflows, it is assumed subsequently that water bodies behave as lakes.

In lakes, morphology is a predominant factor characterizing its stratification. A shallow lake is defined as one where wind energy input prohibits the formation of a stable thermal stratification. The characterization of a shallow lake depends on the combination of fetch and depth. A lake with large area and moderate depth can be considered shallow since the fetch is large enough for wind to maintain mixed conditions. In contrast a deep lake can present isothermal characteristics in a cold season and gradually develop stratification with warming such that in the warmest periods there will always be two distinctive layers: the epilimnion with well mixed conditions, and the hypolimnion with isothermal conditions, but practically thermally isolated from the epilimnion by the metalimnion. It is important to stress that the increase of epilimnion depth depends primarily on solar heating and wind entrainment.

The methodology for generating hypothetical shallow and deep lakes is based on the stratification process. It is assumed that initially the reservoir is fully mixed with temperature T_H and that there is an atmospheric source of heat. As a consequence of heating, a thin surface layer will form with a temperature T_E which is higher than T_H. Wind action on the surface of the lake will lead to a deepening of this thin surface layer and the onset of stratification. Further wind mixing under a continuous source of heat causes a deepening of the warmer top layer, and if this layer of temperature T_E reaches the bottom, stratification is broken and isothermal conditions exist once again.

A lake can be regarded as shallow if stratification can break during a relatively small period of time. To develop a method for identifying shallow lakes from a set of hypothetical lakes, situated in different geographical locations and having different morphometry, the ideas described above are applied in the context of the MIT approach (Octavio et al., 1977). This approach calculates the entrainment of hypolimnetic water into the upper mixed layer on the basis of comparing the rate of change in potential energy of lakes. The formulation suggested in this study is a simplified form of the MIT wind-mixing approach which assumes two distinct lake layers of temperatures T_E and T_H, respectively (see Fig. 6.1). The derivation of the governing equations of the two-layer lake stratification model can be found in the Appendix.

6.2 Generation of Hypothetical Lakes

To determine whether a lake is deep or shallow, using the approach presented above, an indicator that defines the lake type is required. Since in a shallow lake the thermocline moves

downwards relatively fast due to wind-driven mixing, an indicator that defines the mixing stage of a lake can be the percentage ratio of the epilimnion depth to the total lake's depth.

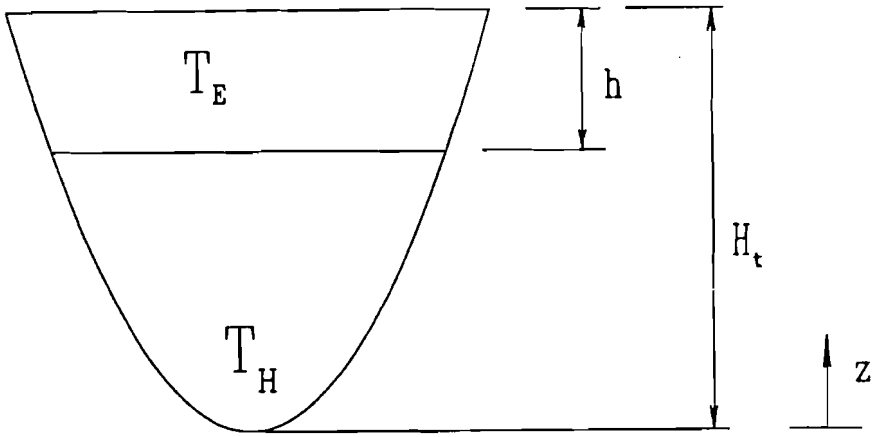

Figure 6.1 Layout of a hypothetical lake morphology and definition of its two layers

Under this definition a shallow lake reaches a 100% mixing ratio in a short period of time, say a month or less. In contrast, a (very) deep lake maintains a mixing ratio close to 0%. Moreover, stratification is more likely to occur during the warmest month within a year, therefore, if a lake becomes fully mixed during the warmest month it is most likely shallow all year round.

With these definitions, determination of hypothetical lakes was performed only for the northern hemisphere under the assumption that southern hemisphere characteristics would be equivalent for longitudinally averaged monthly conditions. The month of July was considered the warmest month in the northern hemisphere. Since wind is the most important force governing mixing within the epilimnion and the movement of the thermocline, it is important to test sensitivities of percent mixing due to wind. For this reason simulations were performed for normal winds (longitudinally historical monthly averages, see Chapter 4), and for an increase and decrease of 50% of normal wind speed.

The surface area of the hypothetical lakes was set to 100 km^2. Linear dependancy between the lake depth and the area of horizontal cross-section was assumed. Five values for lake depth were selected, namely 10, 20, 50, 75, and 150m. Latitudes were changed systematically by 5 degrees. Initial conditions for the simulation were h(t=0) = 0.01 m, T_H = 8 ^oC, and T_E = 8.05 ^oC.

Note that the initial temperature of the epilimnion, T_E, is only slightly higher than that of the rest of the lake, T_H. The initial temperature in this case is nothing more than an arbitrary numerical seed needed to initiate the warming process.

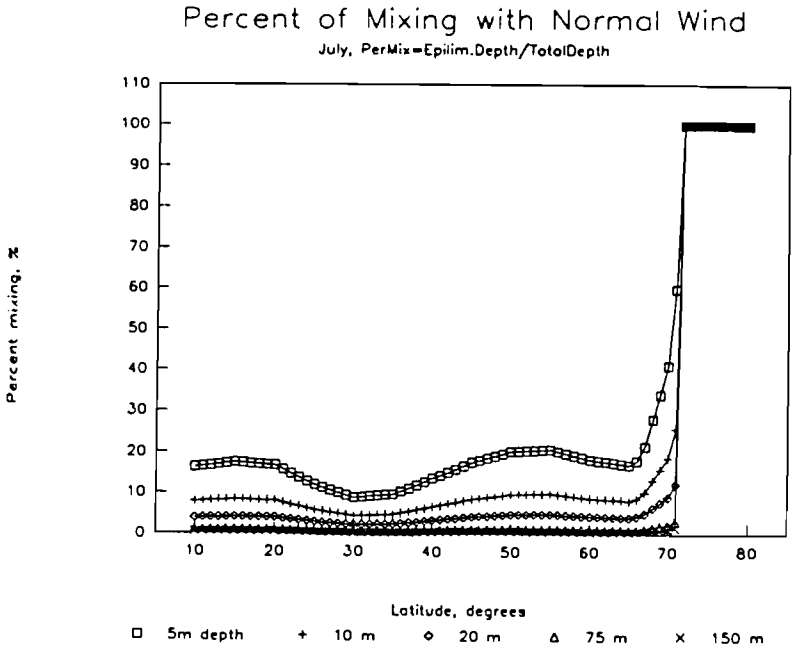

Figure 6.2 Percent mixing vs. latitude for average winds

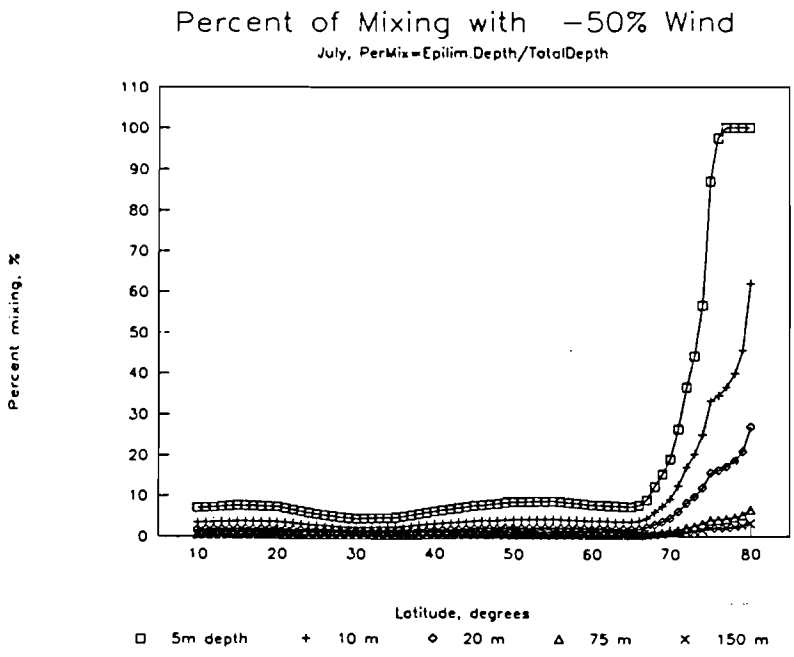

Figure 6.3 Percent mixing vs. latitude for a 50% decrease in normal winds

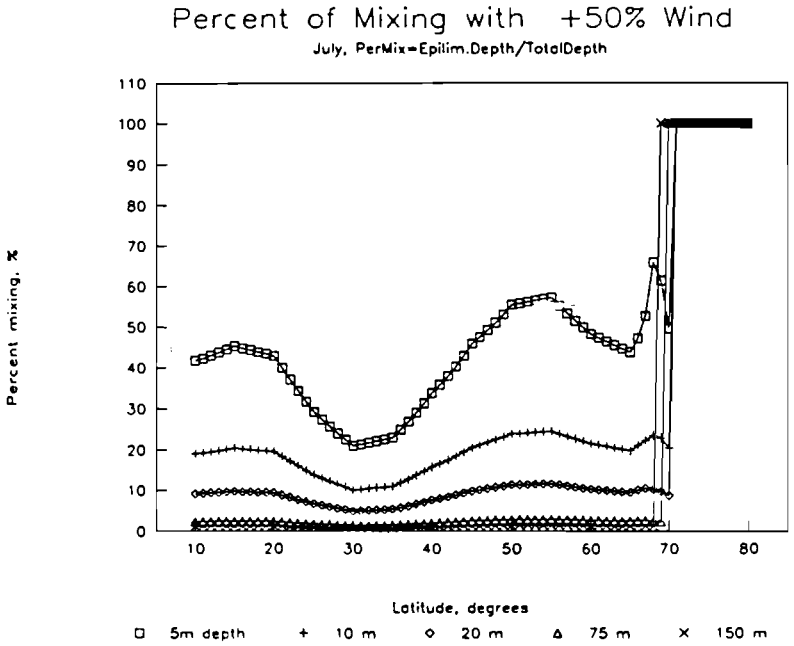

Figure 6.4 Percent mixing vs. latitude for a 50% increase in normal winds

Figures 6.2 to 6.4 show percent mixing vs. latitude graphs for different depths. Comparing the three figures the role of wind is well reflected together with changes along the latitude. The higher the wind speed the higher the percent mixing for a given lake depth. It is also observed that at high and low latitudes percent mixing is high for all depths, characteristic of polar and equatorial regions. In Figure 6.2 isothermal behavior is apparent above 70^{o} depending on depth. There is a tendency of higher stratification around 20^{o} and 70^{o} latitude. From the plots we define lakes with 150 m and 75 m depths as deep since for any wind change the mixing ratio is close to 0%. Lakes of 20 m, 10 m and even 5 m depths can be considered intermediate lakes, while shallow lakes are characterized by less than 5 m depth. For further usage water depths of 75 m, 20 m, and 10 m were selected.

7. IDENTIFICATION OF SENSITIVE REGIONS

7.1 Criteria for Defining Overturn

The definition of overturn is somewhat subjective and can take several forms. Accordingly, four criteria for defining overturn were initially examined:

1. Overturn occurs when more than half of the reservoir exhibits a positive density gradient, a phenomenon that induces convective instability.

2. Overturn takes place when the potential energy of the water column prior to mixing exceeds that of the water column after mixing, i.e., the density profile in the water column is such that the potential energy can be used as a source for turbulent energy generation:

$$P_{bov} - P_{mix} > 0, \qquad (9)$$

where P_{bov} = potential energy before overturn;
P_{mix} = potential energy after mixing.

3. Overturn is assumed when the bottom density is less than the top density.
4. Overturn occurs when the bottom and top density gradients are positive.

Performance of these criteria was tested with two hypothetical lakes, one deep (75 m) and one intermediate (20 m), in a representative middle latitude (55^{o} North). As input, longitudinally and monthly averaged climate data were used (Chapter 4).

Comparison of the overturn criteria for the two lakes are shown in Figures 7.1 and 7.2, indicating the periods of complete mixing (by Julian calendar days). The figures show that the results are similar either for the intermediate or the deep lake. Criteria 1 indicated a somewhat longer period of complete mixing (isothermal conditions) in the late autumn period than did the other three criteria. All criteria indicated the lakes to be dimictic (i.e., two overturns per year), with the longest overturn period occurring in autumn. Since criterion 3 proved to be the most robust and sensitive as well as and physically justified (overturn occurs when the bottom density is less than that at the top), this was accepted for the rest of our study. This criterion is not only indicative of mixing but also indicates persistence of isothermal conditions.

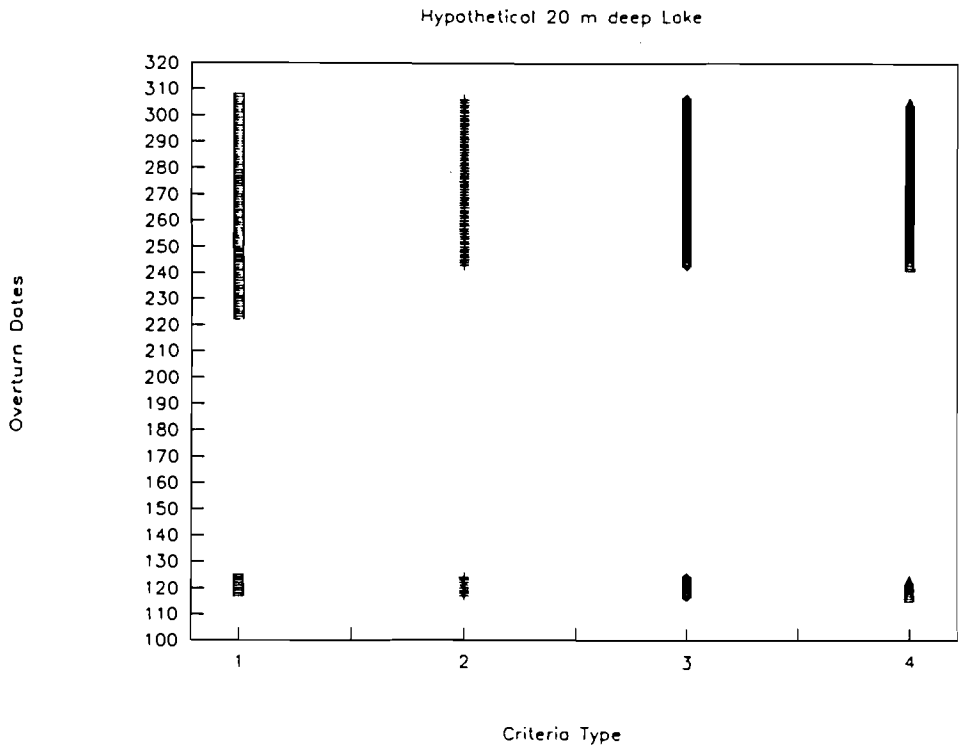

Figure 7.1 Comparison of overturn criteria in an intermediate lake (20 m deep)

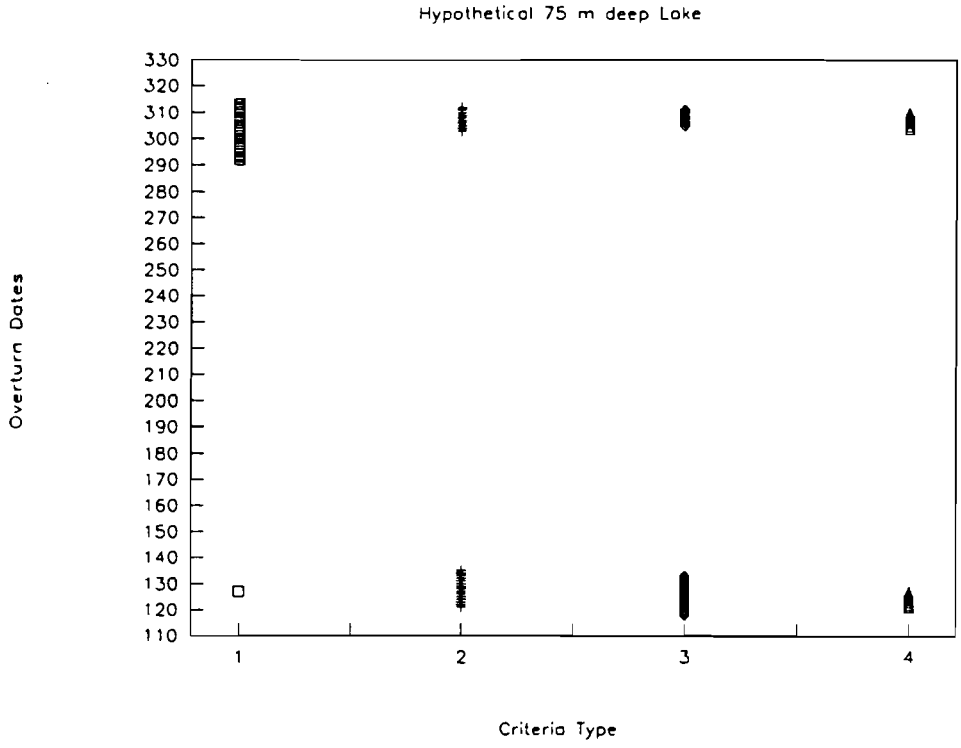

Figure 7.2 Comparison of overturn criteria in a deep lake (75 m deep)

7.2 Sensitivity Analysis

For the purpose of sensitivity studies ±5 ^{o}C alteration was imposed on the longitudinally and monthly averaged historic air temperature (Chapter 4), since this range is characterizing the typical average temperature change induced by the greenhouse effect according to most GCM predictions. The procedure was the same as before but now the IWEP model was used to identify regions of the globe sensitive to climate change.

Simulations were performed for 3 subsequent year periods. The last year results are considered as characterizing "settled" quasy-stable behabior, not dependent on the initial conditions. The results of this last year modelling are further analyzed and presented in Figures 7.3 to 7.15. The general overview of the occurrence of the overturn events during the last modelling year is shown in Figures 7.3, 7.8 and 7.12. If at a certain latitude a lake displays overturn conditions, the corresponding day is marked on the plot with a circle. The overview plots are combining three cases (one base scenario and two sensitivity runs) which differ in the size of the circles. This superimposition allows for instant comparison of the scenarios, albeit somewhat complicating the outlook of the plots. The remaining plots are easier to read: figures 7.4, 7.9 and 7.13 display duration of ice cover persistense with respect to the latitude, and the rest of the plots show duration of the overturn conditions in the lake.
Careful examination of the sensitivity results allow to note the following:

i. The transition latitudes, where lake classification changes from monomictic to dimictic, around 40^{o} N/S, and from dimictic to monomictic, around 70^{o} N/S, are well simulated.

ii. For latitudes higher than 80^{o} the existence of a permanent ice cover (or temperatures close to 0 ^{o}C) does not induce overturn.

iii. Stratification in shallow and intermediate lakes was slightly sensitive to changes in air temperature in subtropical regions. On the other hand, stratification of deep lakes, was significantly sensitive to air temperature changes in this same region. In temperate and polar regions the sensitivity of lake stratification to changes in air temperature was important for all lake depths.

iv. As expected in all cases, during warming events turnovers occur earlier in the year. During cooling turnovers are delayed.

v. Sensitivity of duration of stratification in subtropical intermediate and shallow lakes is small, while it is considerable in a deep lake. In contrast, the sensitivity is equally significant for all lake depths in temperate to polar regions.

vi. Sensitivity of the duration of freezing period is greater in the range of latitudes 70^{o} to 80^{o} (subpolar and polar zones) than in the 50^{o} to 70^{o} latitude range (temperate zone), regardless of lake depth. In the subtropical zones, ice cover duration is more sensitive in the deeper lakes than in the shallower ones.

vii. In the 10 m deep lake, as shown in Figure 7.3, the lower latitudes (0^{o} to 30^{o}) develop isothermal conditions for most of the year, most likely because there is not enough heating or cooling to induce stratification except for short periods in the summer. The duration of turnover occurrence can change by 10 to 60 days in middle latitudes (40^{o} to 70^{o} latitude range). At the 40^{o} latitude, for example, the turnover period increases by as much as 60 days with an 5 ^{o}C increase in air temperature. At this same latitude the turnover period decreases by 40 days in the case of 5^{o} cooling. As shown in Figure 7.4, the surfaces can be ice covered from latitude 37^{o} and higher under normal conditions. The same figure shows that cooling would produce a shift in which ice cover can begin at lower latitudes, and warming would produce the opposite effect. Shift in ice formation towards lower latitudes is evidenced through a reduced overturn period at the 35^{o} latitude. At the 75^{o} latitude turnover is entirely suppressed by cooling. In contrast, at the 80^{o} latitude dimictic conditions are induced under warming, when under normal conditions the system is amictic. Figure 7.5 shows that the duration of summer stratification can mostly be altered in high latitude ranges, reducing it under cooling and increasing it under warming. Figures 7.6 and 7.7 further verify that at lower latitudes there is a potential for stratification to shift towards the winter season under warming.

viii. In the 20 m deep lake (see Figure 7.8) changes are more pronounced than those of a 10 m deep lake. The winter turnover is altered at latitude 35^{o} under cooling, changing conditions from monomictic to dimictic. This phenomenon can be partly explained by Figure 7.9, where it can be seen that under cooling ice covered surfaces appear at lower latitudes. Changes in turnover duration can fluctuate from 4 to 40 days in middle latitudes (30^{o} to 70^{o} latitude range). Warming, on the other hand, generally increases the duration of overturn periods. At latitude 75^{o}, while cooling suppresses overturn resulting in an amictic lake, warming produces an extra overturn period converting the lake to a dimictic one. Figure 7.10 shows that the duration of summer stratification generally increases with warming and decreases with cooling. The latter is verified by Figure 7.11, which shows the times within the

year at which summer stratification begins and ends. As in the 10 m deep lake, stratification periods occur earlier in the year, towards the spring season, in the low-latitude ranges.

ix. Results for the 75 m deep lake are shown in Figure 7.12. Low latitudes show stratified conditions all year round, due to the combination of the large lake depth, which seems to sustain a metalimnion, and the initial water temperature condition (4 ^{o}C), perhaps too cold for warmer surface waters to reach the bottom. Changes begin to occur at latitude 30^{o}, where under cooling, amictic lakes have the potential to become monomictic. At latitude 40^{o} dimictic conditions could occur under cooling. In middle latitudes the duration of overturn can change by up to 10 days. What seems to be more important is the shift in the times at which overturn occurs. As in the previous cases, at the latitude range of 75^{o} to 80^{o} warming has the potential to produce dimictic conditions (amictic otherwise). Figure 7.13 consistently shows that ice cover duration decreases under warming and increases under cooling. Formation of ice covered surfaces shifts southward under cooling and northwards under warming. Figure 7.14 shows a consistent pattern of longer stratification periods under warming, the reversed phenomenon occurs under cooling. The latter is ratified by the times at which summer stratification begins and ends, as shown in Figure 7.15.

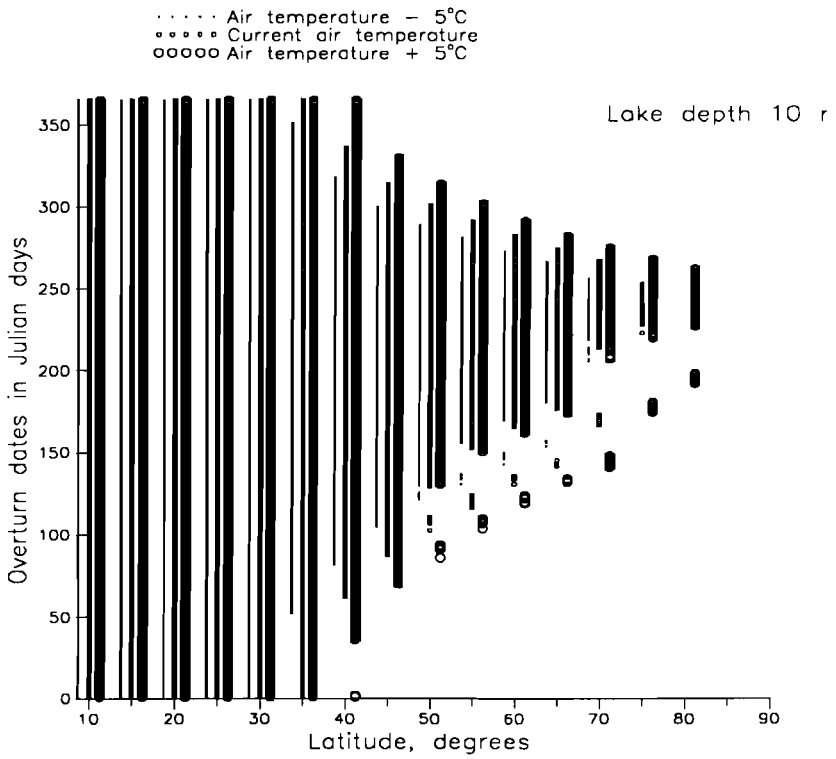

Figure 7.3 Overturn results for a 10 m deep lake under a ±5 ^{o}C air temperature change

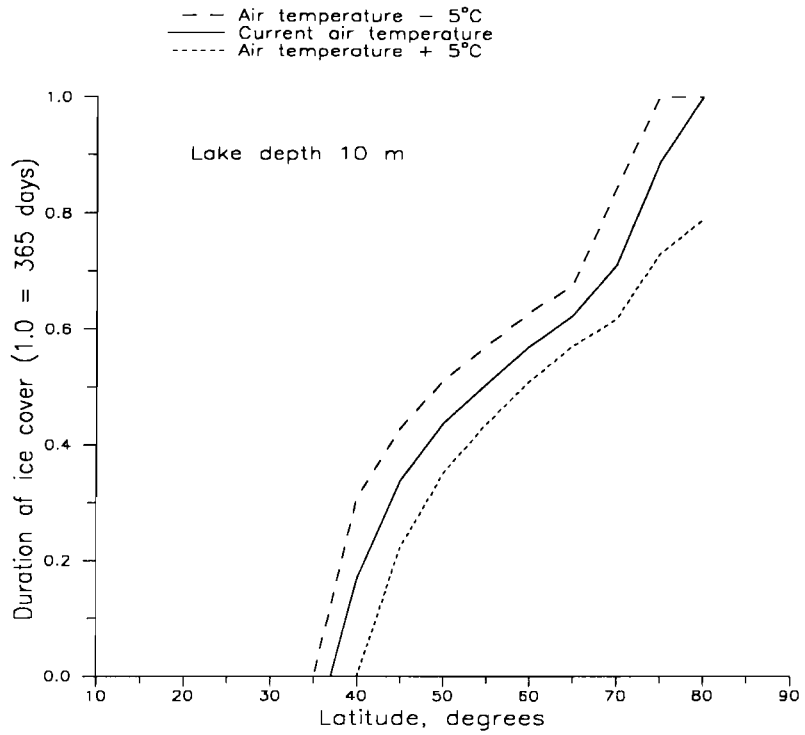

Figure 7.4 Duration of ice cover, 10 m deep lake

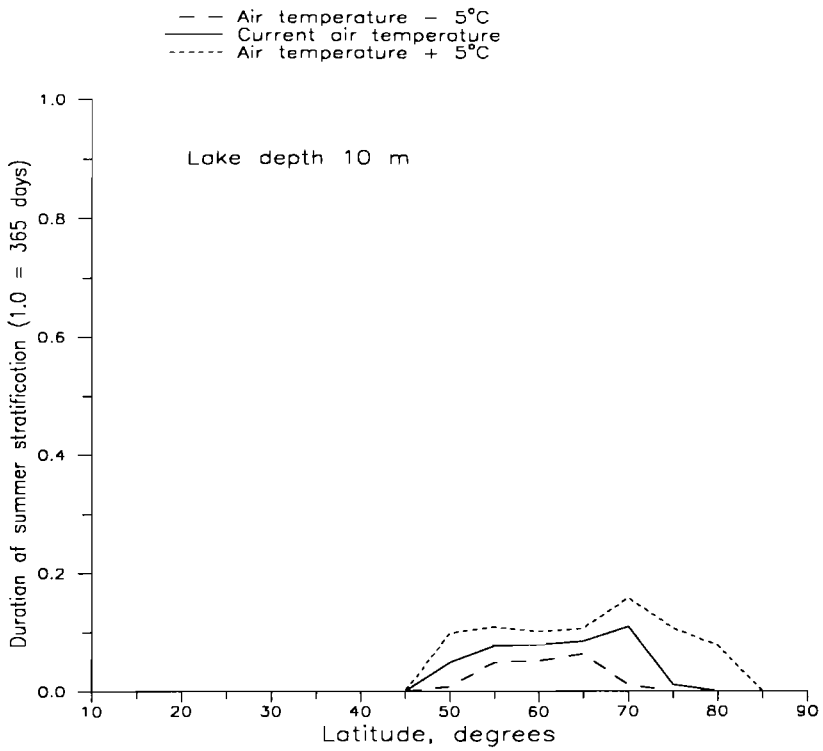

Figure 7.5 Duration of summer stratification, 10 m deep lake

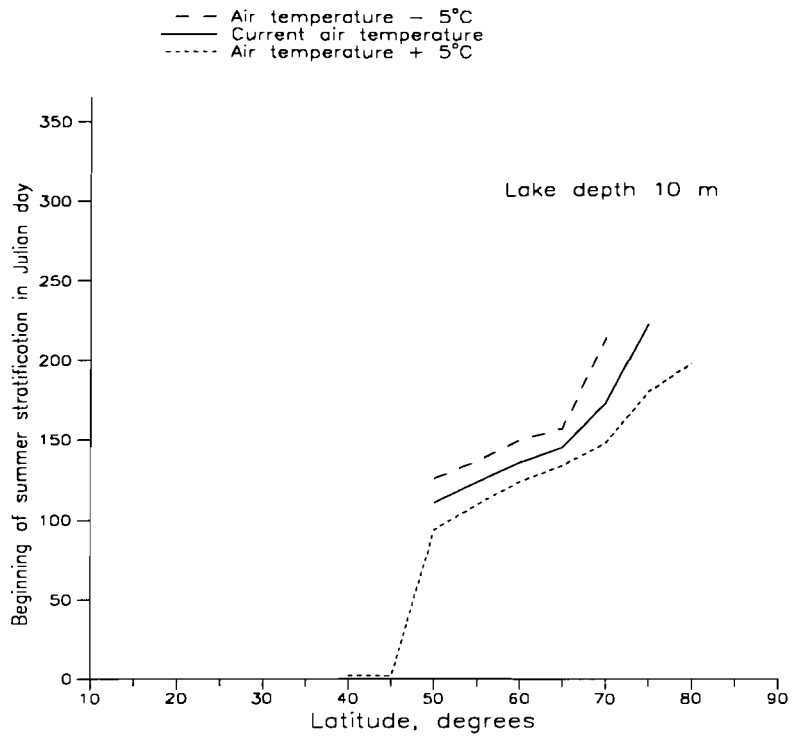

Figure 7.6 Beginning of summer stratification, 10 m deep lake

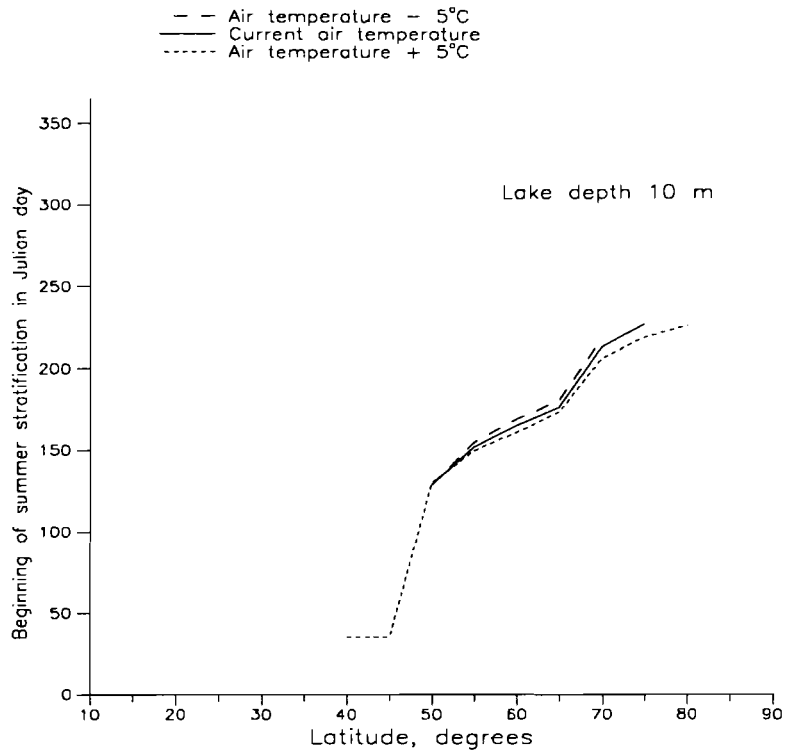

Figure 7.7 End of summer stratification, 10 m deep lake

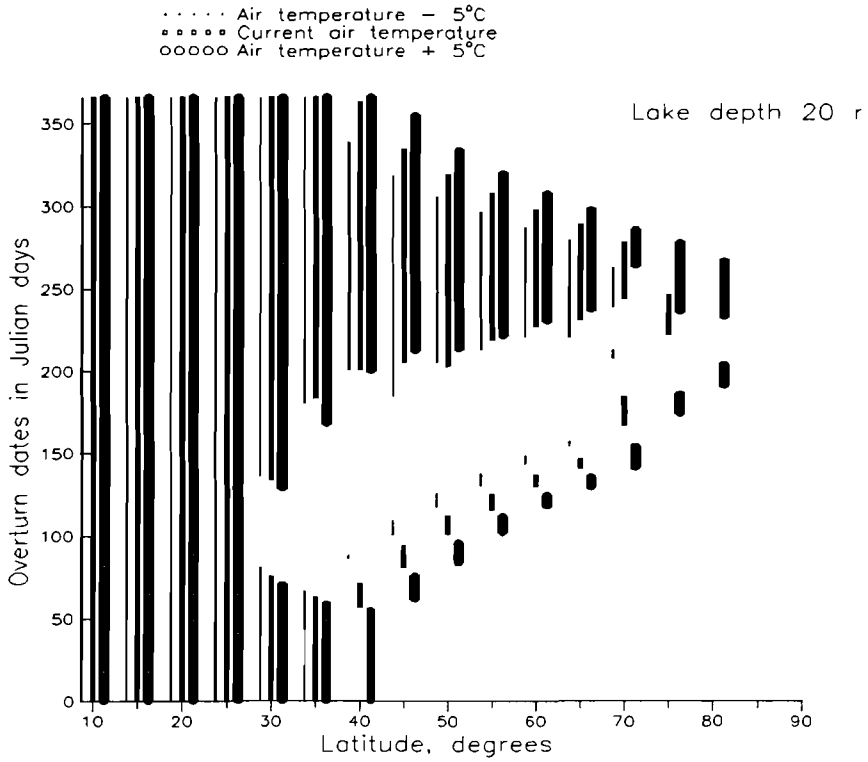

Figure 7.8 Overturn results for a 20 m deep lake under a ±5 °C air temperature change

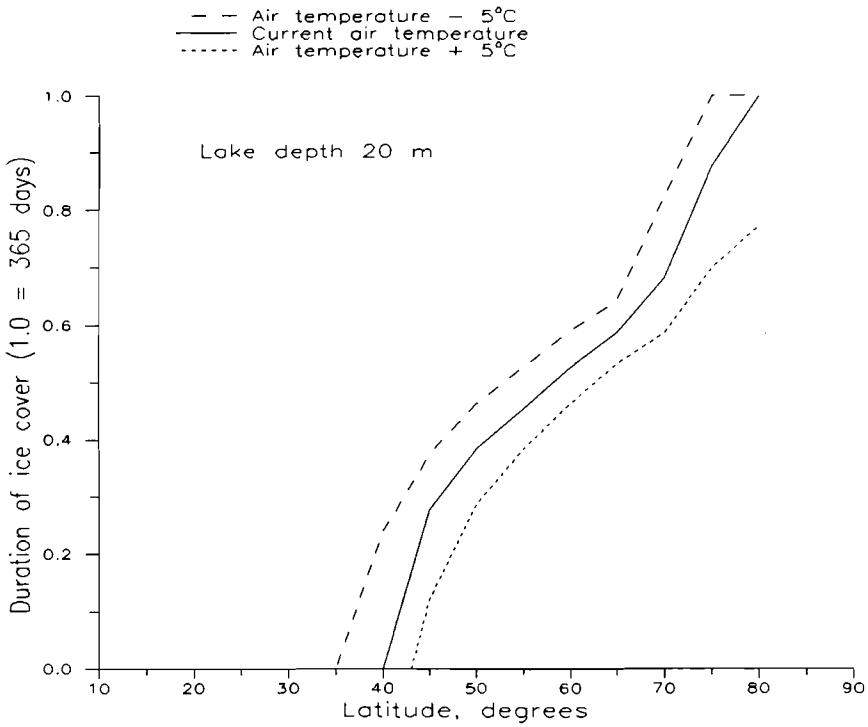

Figure 7.9 Duration of ice cover, 20 m deep lake

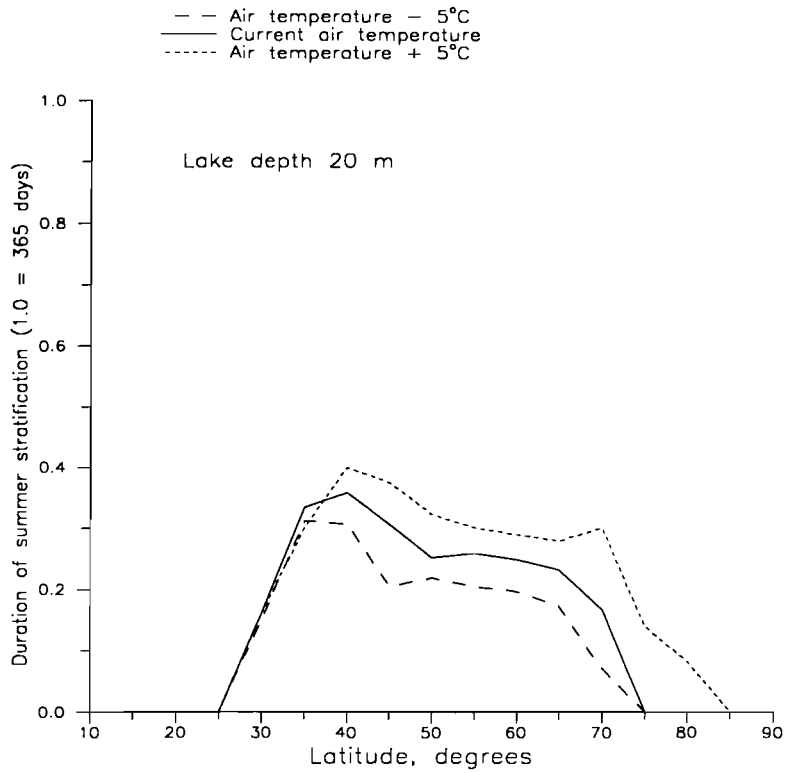

Figure 7.10 Duration of summer stratification, 20 m deep lake

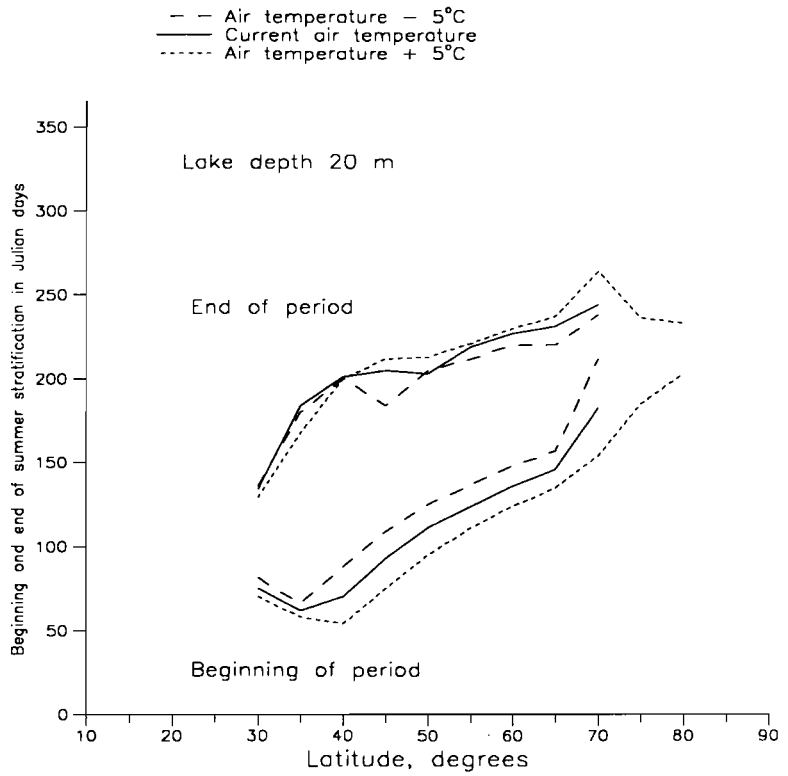

Figure 7.11 Beginning and end of summer stratification, 20 m deep lake

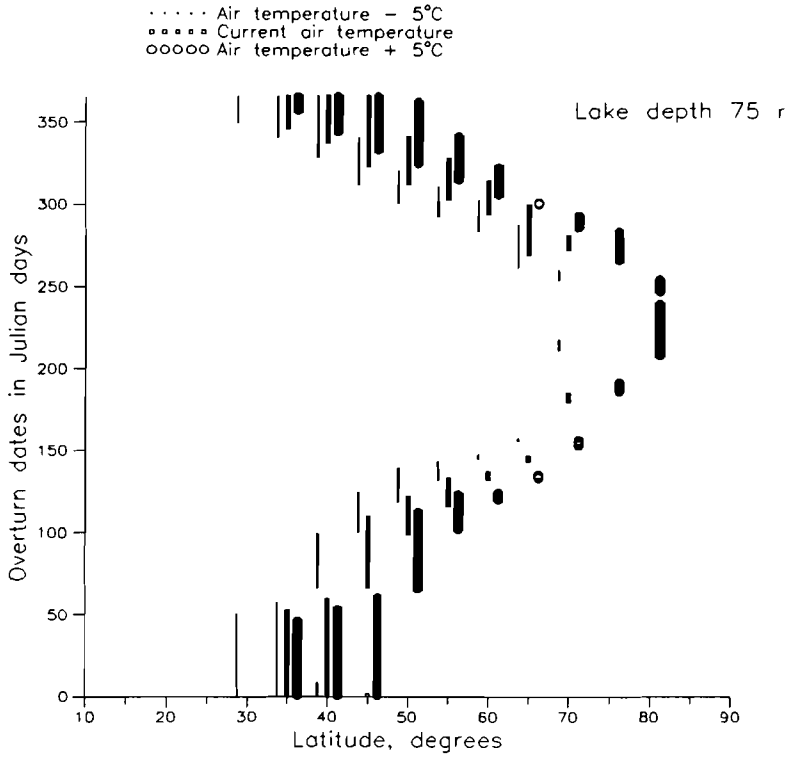

Figure 7.12 Overturn results for a 75 m deep lake under a ±5 °C air temperature change

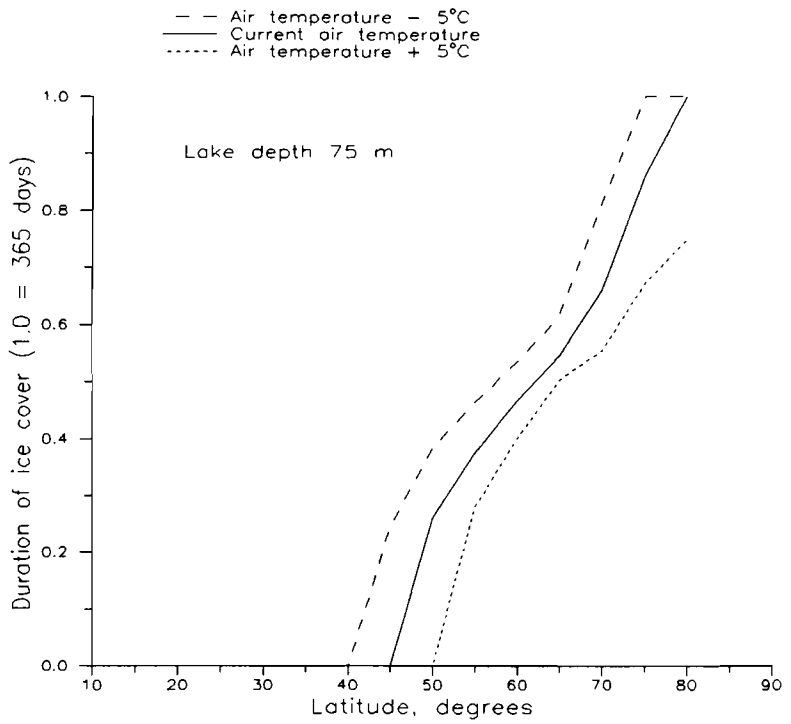

Figure 7.13 Duration of ice cover, 75 m deep lake

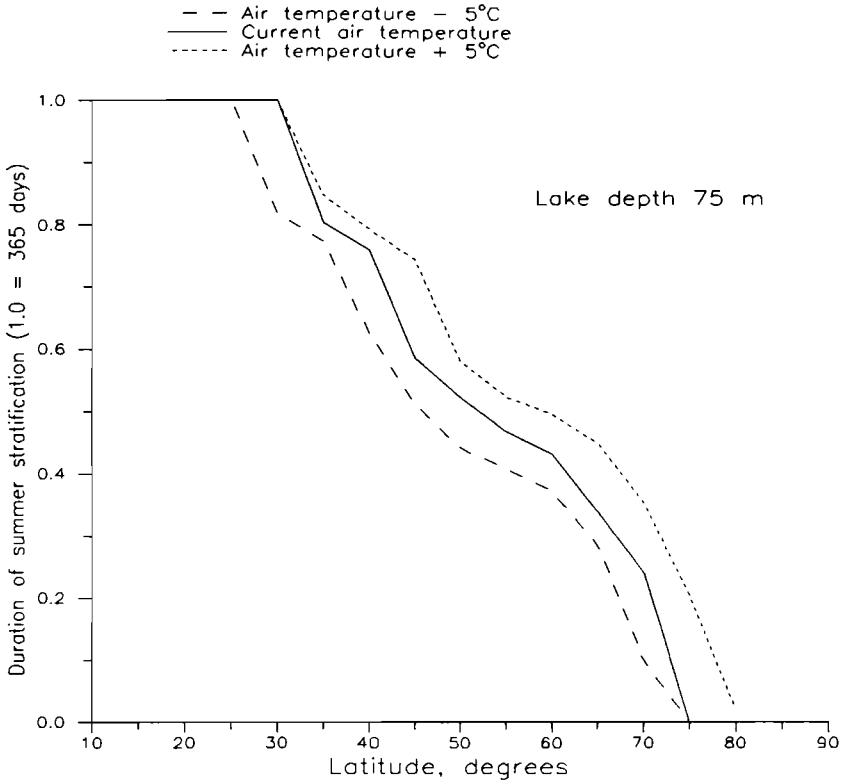

Figure 7.14 Duration of summer stratification, 75 m deep lake

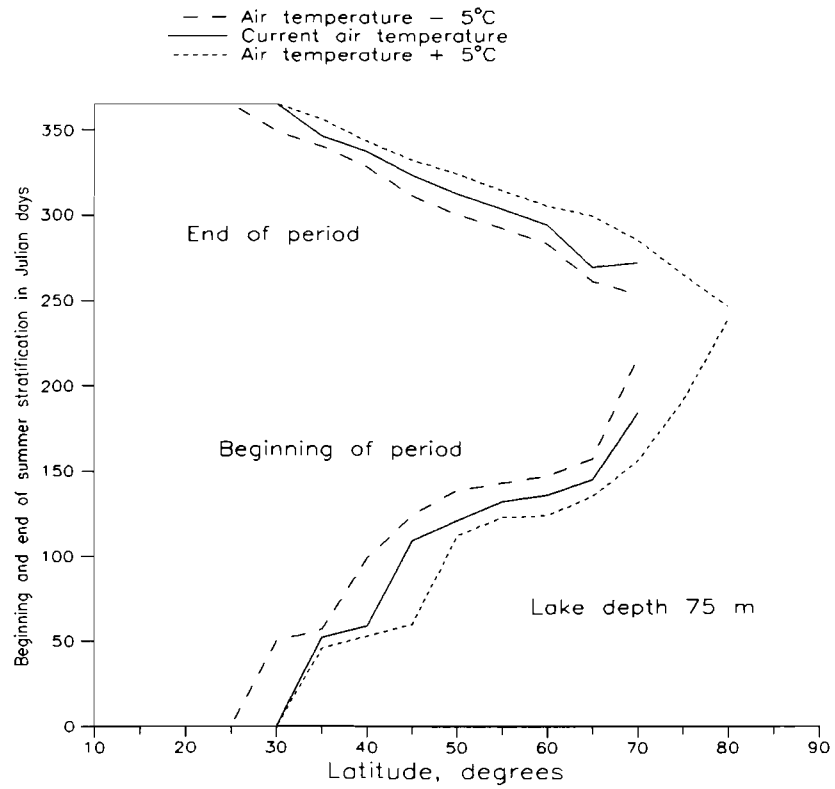

Figure 7.15 Beginning and end of summer stratification, 75 m deep lake

7.3 Concluding Remarks

The results suggest that the sensitivity of lakes to changes in air temperature greatly increases in geographic regions where lakes change stratification patterns from warm monomictic to dimictic (about latitude 40^{o}), or from dimictic to cold monomictic (about latitude 70^{o}), referred to as transition regions. The latter condition is expected due to the non-linear nature of the system which is known to be highly sensitive near transition points. Changes in overturn periods by as much as 10 days, common for changes of 5 ^{o}C in air temperature, can be important particularly in eutrophic lakes. A 10 day increase in overturn duration could enhance algal growth due to longer exposure of the algal cells to light and the availability of nutrients brought to the surface during the turn over. On the other hand, lengthening stratification periods would extend periods of anoxic bottom conditions that would enhance nutrient releases from decaying material, which in the next overturn occurrence would be recycled through the lake thereby enhancing eutrophication.

As a result of the above findings, we have chosen to define the transition regions as sensitive belts of the globe, with latitudes ranging from 30^{o} to 45^{o} N/S and 65^{o} to 80^{o} N/S. These results shall be evaluated mainly as indicators of potential changes in the stratification pattern of lakes. In order to provide more accurate assessments, improvements still need to be made in the criterion defining the occurrence of turn overs by relaxing or improving its mathematical representation (taking into account bounds of numerical errors). The initial conditions should be revised, especially for deep lakes at low latitudes, specifying more realistic initial bottom temperatures.

8. SIMULATION OF THE BEHAVIOR OF REAL LAKES

8.1 Real Lakes Selected for Simulation

It is difficult to identify real lakes with the required geomorphological information located precisely within the bounds we have established. Thus, we have relaxed the limits somewhat to include a representative set of real lakes. Table 8.1 presents the selected lakes along with the basic geomorphological characteristics (depth, surface area, and volume). We refer to the selected water bodies as lakes, since they were treated as having negligible inflow.

8.2 Simulation Results

Simulations were performed to assess changes in the stratification patterns of real lakes due to climate change. The availability of high quality data collected by the International Lake Environment Committee, ILEC, (UNEP, 1987-1990), made it possible to perform consistent simulations.

Lake morphometry was approximated with a power function dependent on surface area A_o and depth z: $A = A_o z^k$. The power k was calibrated to match the lake morphometry data (volume, maximal depth and the surface area).

For the base case scenarios, i.e., existing climate conditions, simulations were performed on an average monthly basis using historical data. The data sets used were those of the climatological station nearest to the lakes (see Chapter 4).

For analyzing the impact of global climate change, the scenario of doubling in the concentration of atmospheric CO_2, and the corresponding GFDL climatological model results were used. As noted earlier, temperature change was considered alone (representing a conservative approach). The GFDL temperature differences were interpolated linearly to the station location and added to observed data (see Section 4.3). This is found to be a better practice than directly using GCM temperature results (see for example Lettenmaier and Gan, 1990). All other meteorological variables (relative humidity, wind speed and cloudiness) were kept unchanged. One reason for that is the key role which air temperature plays in the heat balance of the lake. Besides, there is no clear translation procedure which could lead from the GCM grid data to changes in local meteorology necessary to calculate the waterbody heat household.

Simulations were started on June 1 with an arbitrary initial condition of isothermal profile $4^{o}C$. As mentioned previously, simulations for each lake were performed for three consecutive years. Since the same meteorological conditions were periodically applied each year, quasi-steady-state heat balance was reached and results of the last year simulations were used for the analysis. The effect of the initial conditions on the periodically stabilized solution was not significant.

Impacts of climate change were measured through changes in i) overturn occurrence, where overturn is defined as in Chapter 7; ii) changes in the number of days with ice cover; and iii) changes in the duration of stratified periods. The plots 8.1 through 8.9 represent the overview of the seasonal evolution of lake condition defined by overturn events and ice cover, occurrence of which is marked with the corresponding symbols. The air temperature displacement with respect to the base case is displayed on the vertical axis. Such plot layout allows for comparison of the lake behavior patterns in the cases of the base scenario and the scenario derived from the GCM results. At the same time one can get an idea about the extent of changes in the regional climate which is causing these behavior alteration. Results of the nine case studies follow.

Case study 1: Shasta Lake

Shasta Lake, on the Sacramento River, is a major source of water supply to the state of California. Under present conditions the water delivered from Shasta Lake for most beneficial uses downstream is of high quality. The major quality problem at present is temperature which, if high enough, can detrimentally impact cold water habitat. Recent studies have demonstrated that stream temperatures in the Sacramento River are controlled by the availability of cold water in upstream reservoirs, e.g. Shasta Lake, and management of these reservoir (Orlob et al., 1990). Ongoing research on the impacts of global climate change on the water quality of Shasta lake, makes this case study an interesting one to analyze, despite its short resident time (0.5 year, on the average).

Table 8.1 Lakes Located at Sensitive Latitudes

NAME	LATITUDE (degrees)	APPROXI-MATE LONGITU-DE (degrees)	DEPTH* (m)	SURFACE AREA (km^2)	VOLUME (km^3)
Shasta Lake (California, USA)	42 N	122 W	184 (SH)	120	5.5
Great Bear Lake (Northwest Territories, Canada)	66 N	120 W	149 (mean)	31,153	2236.0
Lake Seneca (New York, USA)	43 N	77 W	198 (max)	175	15.5
Ezequiel R. Reservoir (Neuquen Province, Argentina)	40 S	66 W	60 (SH)	816	20.2
Lake Geneva (Switzerland and France)	46 N	6 E	310 (max)	584	88.9
Lake Maggiore (Italy and Switzerland)	46 N	8 E	370 (max)	212	37.5
Changshou-Hu Reservoir (Sichuan Province, People's Republic of China	30 N	107 E	34 (SH)	60	0.7
Ladoga Lake (Russia)	60 N	31 E	230 (max)	18,135	908.0
Lake Biwa-Ko (Shiga Prefecture, Japan)	35 N	136 E	104 (max)	674.4	27.5

* For lakes, the depth is the mean or maximum depth.
For reservoirs, the depth is the structural height (SH) or mean depth.
Source: Data Book of World Lakes Environment (UNEP, 1987-1990)

Base case simulation results indicate that the lake has an overturn period from December to March (see Figure 8.1). Observations show that the reservoir is isothermal from January to March. Thus Shasta Lake can be classified as a warm monomictic. The discrepancies between simulation results and observations can be partly explained by the fact that this study used a meteorologic station located about one degree north of Shasta Lake, in a colder watershed.

Under changed climate conditions, simulation results show that the isothermal period disappears, thus the reservoir remains stratified all year round. These results agree with recent investigations where it has been shown that under global climate change the isothermal conditions are reduced to the month of January, and part of February (Meyer and Orlob, 1992), and water temperature increases year-round. The increase temperature poses a threat

to the survival of cold water habitat already in stress. Moreover, the consequences of high temperatures, such as lower dissolved oxygen concentration at saturation and changes in the reaction kinetics of nutrients and biota are likely to enhance eutrophication.

Case study 2: Great Bear Lake

Great Bear Lake is the largest lake in Canada. The residence time of this lake is 124 years. Therefore, neglecting through flow in the lake is a justified assumption. The meteorological data used for simulation of present conditions was that of the Aklawik meteorological station because of the completeness of the data, although the station at Port Radium is closer to the lake.

Figure 8.2 shows the simulation results for this lake. Simulations of present conditions were in general accordance with observed data. According to observations, the lake is ice covered from November to July (UNEP, 1987-1990), while our study resulted in the period from September to July. This can partly be explained by the fact that the Aklawik station, located to the north, has lower average annual air temperatures (-9.2 ^{o}C) than those at the Port Radium station (-7.2 ^{o}C). Under present climate conditions the simulation indicates that overturn periods do not occur. According to existing observations the lake experiences complete circulation only one year out of three. It is therefore classified as cold monomictic.

Under changed climatic conditions, simulations indicate a reduction in the period of ice cover from 82% of the year to only 65%. As a result of prognostical air temperature increase, which can reach as much as 9 ^{o}C as it is shown in Figure 8.2, strong convective mixing occurs in spring and autumn. The latter condition implies that the lake can potentially become dimictic, with hydrophysical features typical of temperate lakes.

Case study 3: Lake Seneca

Lake Seneca is the largest of a group of long and narrow lakes in west New York State known as the Finger Lakes. Observations indicate that the lake has a residence time of 18 years, long enough to neglect through flows. On an average year the lake is not ice covered, and present stratification patterns classify the lake as monomictic. Simulations resemble these observations (see Figure 8.3). Global warming simulations did not reveal substantial changes, thus the lake will remain monomictic without ice cover.

Case study 4: Ezequiel Ramos Reservoir

Ezequiel Ramos Reservoir is a multi-purpose impoundment used for water supply, transportation, recreation and fisheries. The lake is subject to convective overturns in winter, classifying it as warm monomictic. This overturn period maintains high dissolved oxygen concentrations at all depths. Present case simulation results resemble the monomictic character of the lake. The future climate scenario revealed no change in the stratification pattern, thus present circulation conditions are expected to hold in the future.

Case study 5: Lake Geneva

Lake Geneva is a major source of water supply. Eutrophication has recently been noticed resulting in low dissolved oxygen concentrations, particularly in deep lake layers and anoxic

bottom conditions during most part of the year (Lachavanne,1980). The residence time of the lake is 12 years.

In accordance to existing observations, present case simulations indicate that the lake is classified as warm monomictic, with a turnover in spring time (see Figure 8.5). Our simulations show that the assumed future climatic change will suppress the spring overturn, which gives the lake a new classification of warm monomictic. This result implies that under changed climate enhancement of anoxic bottom conditions and further eutrophication of the lake are likely.

Case study 6: Lake Maggiore

Lake Maggiore is classified as warm oligomictic. Our simulations show that overturns do not occur under present conditions (see Figure 8.6), in accordance to limnological observations. Global climate change simulations do not indicate changes in lake stratification pattern as well.

Case study 7: Changshou-Hu Reservoir

Changshou-Hu Reservoir has multiple uses: transportation, hydroelectric power, water supply, and fishery. As adequately produced in our simulations, this lake is classified as warm monomictic, subject to winter convective overturns from December to February (see Figure 8.7). Under future climatic conditions simulation results reveal no potential changes in lake stratification pattern.

Case study 8: Lake Ladoga

Lake Ladoga is the largest European freshwater body. It has a residence time of 12.3 years. The current lake stratification pattern classifies the lake as dimictic. The lake is frozen from February to May. Overall, these characteristics are well reflected by our computations, albeit simulations reveal ice cover begins in January, a month earlier. This discrepancy can largely be explained by the fact that the meteorological station used for simulations, Petrozavodsk, is located in a colder area and has a lower annual average temperature (2.4 ^{o}C), than Sucho Island station (3.2 ^{o}C), which is located closer to the lake but has insufficient data.

The simulation results under changed conditions, which can imply an increase in air temperature up to 7 ^{o}C, reveal several features. First, no ice cover might be present. Second, the lake will remain dimictic. Intensive cooling during winter will lead to inverse stratification during March and April, late autumn and winter. Third, summer stratified conditions seem to be preserved as at present. If the simulated future changes take place, environmental conditions will inevitably be affected. The absence of ice cover in winter can potentially stimulate fog formation with a subsequent increase in moisture content in the air. The lake's biota, which presently has a number of unique species, might also be impacted by the absence of ice cover. Convective mixing can potentially have more significant consequences due to the longer duration of overturn periods.

Case study 9: Lake Biwa-Ko

Lake Biwa-Ko is Japan's largest lake, which supplies water to 13 million residents in the

Osaka/Kyoto/Kobe megalopolis. Water quality of the lake is thus a serious concern. The lake is formed by two distinct water bodies, called the Northern Lake, with a mean depth of 3.5 m and a residence time of 0.04 years, and the Southern Lake, with a mean depth of 104 m and a residence time of 5.5 years. The lake shows a distinct trend towards eutrophication.

Due to the long residence time of the Southern lake, it is the only one considered for simulations, allowing the neglecting of through flows. Presently the lake is classified as warm monomictic, as our simulations reproduce (see Figure 8.9). Convective mixing occurs during January, February and March, and stratified conditions prevail from May to December. Simulations under climatic change revealed no significant change in the stratification pattern.

8.3 Concluding Remarks

The results indicate that there is a potential for lake classification to be altered due to global warming. The impacts on each lake studied were different depending on their geomorphologic characteristics and their location. For this reason five of the nine lakes experienced no significant change in stratification patterns under changed climatic conditions. For example, the stratification patterns of the polar lakes responded differently under global warming. For the Great Bear Lake, a very large cold monomictic lake, the possible increases in air temperatures up to 9 ^{o}C reduced ice cover enough to induce circulation and reclassifying the lake as dimictic. In Lake Ladoga, a large but smaller water body than Great Bear lake and dimictic, temperature increases up to 7^{o} C made ice cover disappear completely but intensive cooling in winter led to longer turnover periods maintaining the dimictic character. In conclusion, even though the transition regions are believed to be regions where stratification patterns are affected the most, the response of a lake to global climate change can be other than only impacts on its mixing classification, responses also include impacts in characteristics such as ice formation, or overall water temperature changes.
In general, the warmer climatic conditions predicted by the GFDL model led to lake reclassification representative of lower latitudes. For example, Great Bear Lake, presently a subpolar cold monomictic lake, can potentially acquire the characteristics of a dimictic temperate lake. Lake Geneva, presently a warm monomictic lake, can become oligomictic. Lake Shasta, presently a warm monomictic lake, can become amictic.

It should be noted that even if there was no change in stratification pattern, as in the cases of Lake Ladoga, Ezequiel Ramos Reservoir, Lake Maggiore, Changshou-Hu Reservoir, and Lake Biwa-Ko, water temperature changes can be significant enough to generate changes in water quality, biota, and the surrounding environment. The absence of an ice cover in Lake Ladoga, for example, represents an immediate impact in local climate by the enhancement of fog formation.

These results should be interpreted only as a first step in identifying potential impacts of global climate change on the stratification pattern, and consequently on water quality of lakes. The major restrictions of this study are: i) the limitations of the overturn criterion used, as explained in Section 7.3; ii) the use of only one GCM dataset, and the uncertainties involved in GCM outcome; iii) use of the averaged meteorological data from the stations, thus taking out of consideration the variability of local climate.
Climate change effects on overturn periods and stratification should be further analyzed including climatic variables other than air temperature and including realistic hydrologic boundary conditions. From the water quality point of view, investigation of possible

alterations should be examined through monitoring, experiments, and a formalized modeling effort which accounts for changes in the ecological processes that govern water quality.

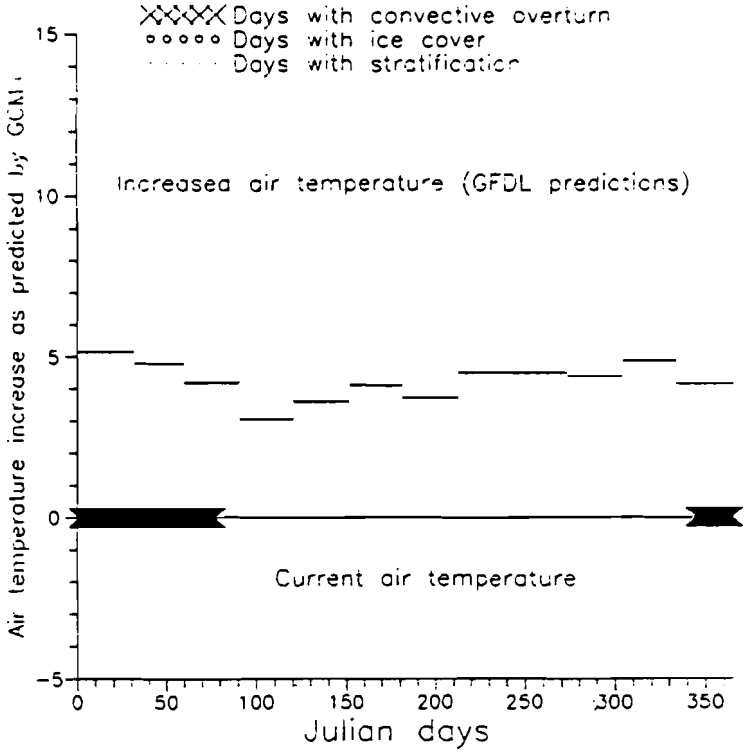

Figure 8.1 Shasta Reservoir, California, U.S.A.

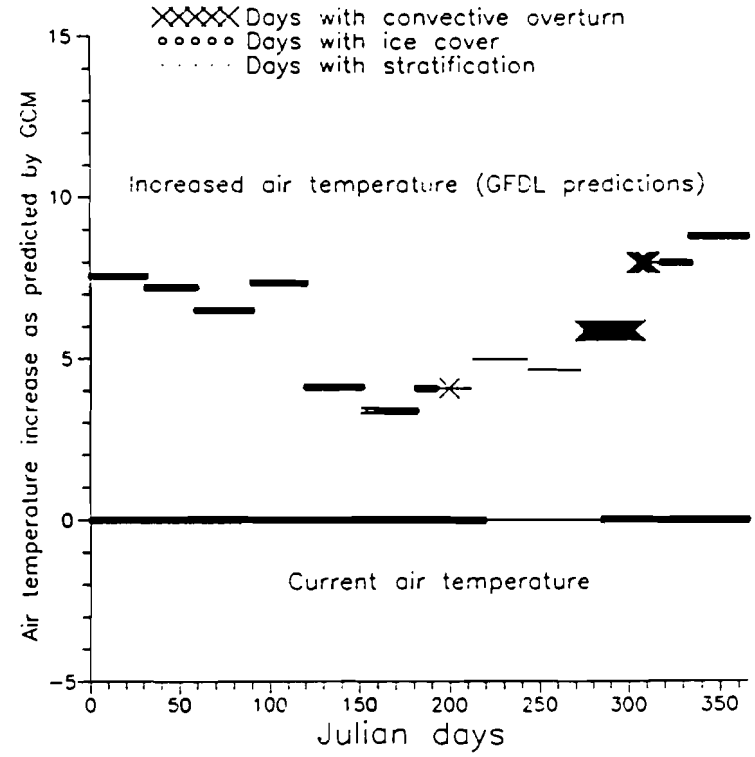

Figure 8.2 Great Bear Lake, Northwest Territories, Canada

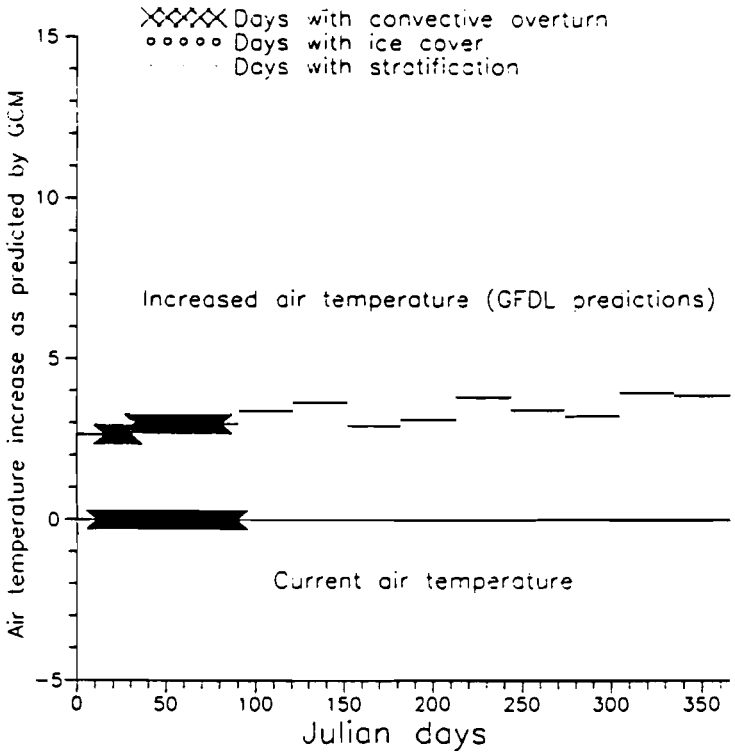

Figure 8.3 Lake Seneca, New York, U.S.A.

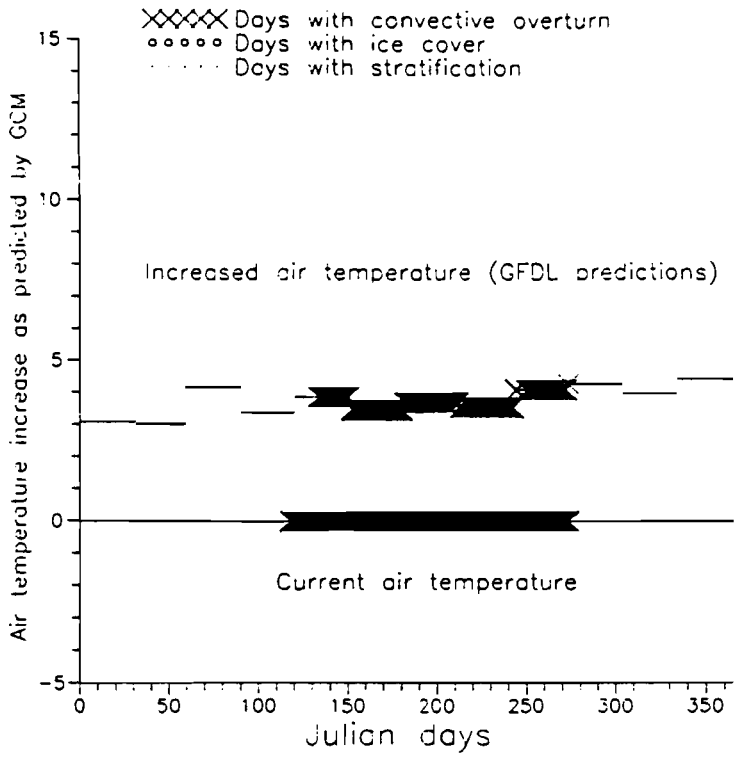

Figure 8.4 Ezequiel Ramos Reservoir, Neuquen, Argentina

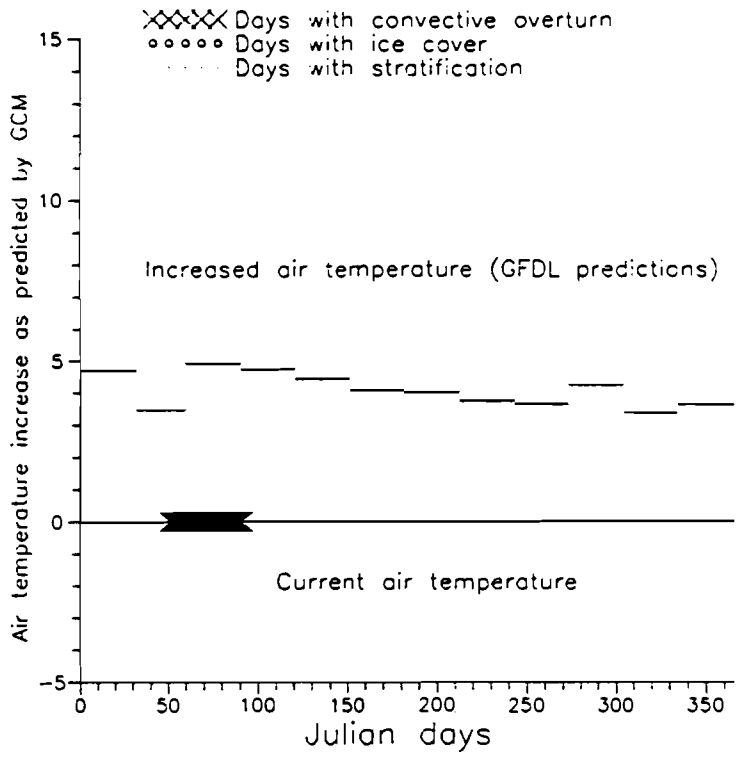

Figure 8.5 Lake Geneva, Switzerland and France

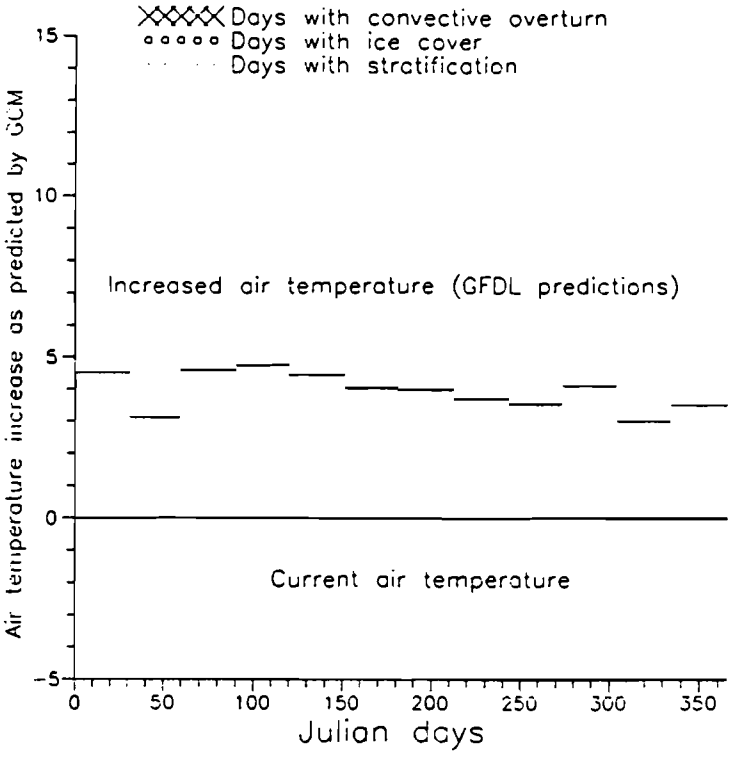

Figure 8.6 Lake Maggiore, Italy and Switzerland

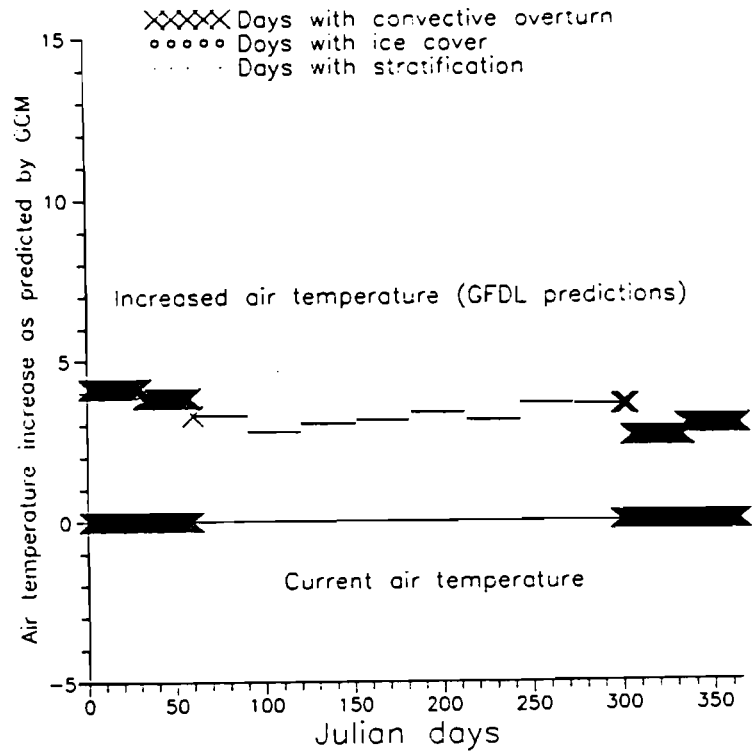

Figure 8.7 Changshou-Hu Reservoir, People's Republic of China

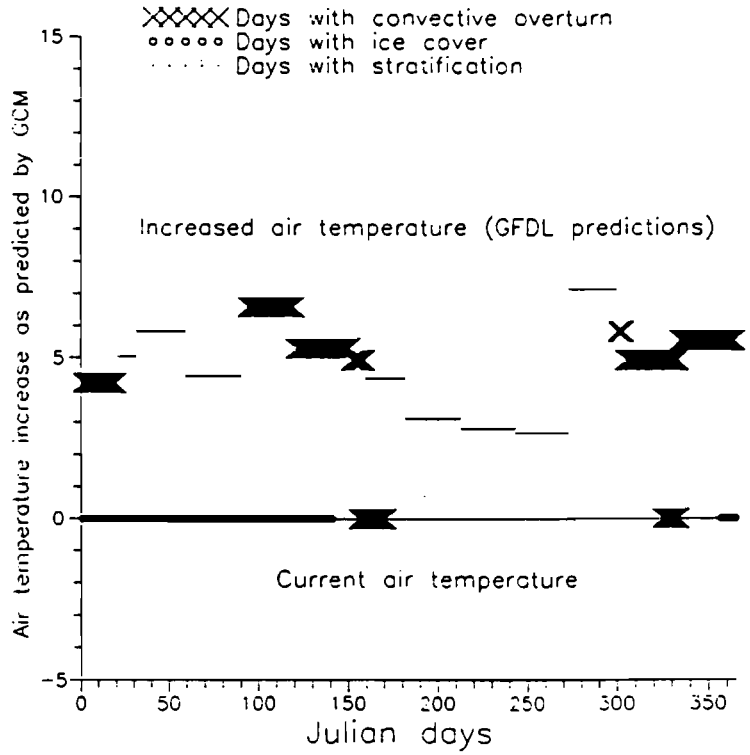

Figure 8.8 Lake Ladoga, Northern Russia

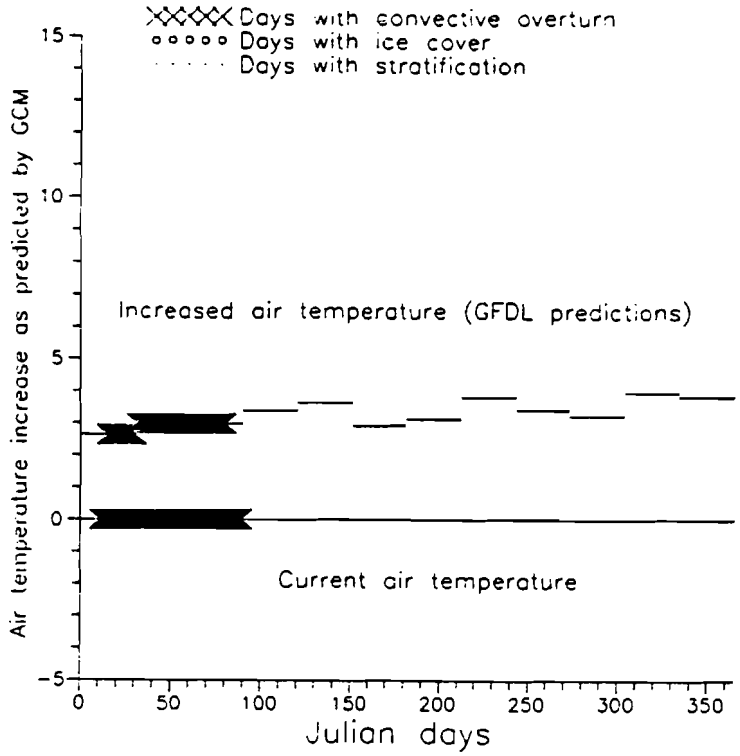

Figure 8.9 Lake Biwa-Ko, Shiga Prefecture, Japan

9. SUMMARY AND CONCLUSIONS

This study presents the findings of a systematic assessment on potential impacts of global climate change on lake hydrothermal dynamics, including modifications to thermal energy budget and stratification patterns, both of which can strongly influence water quality. The study identifies lake morphometry and geographic location as critical factors affecting lake response to climate change.

A vertical one-dimensional model developed at the Institute for Water and Ecological Problems of Russia (IWEP) was used to analyze vertical and temporal changes in lake hydrothermal dynamics. Performance of the IWEP model was compared to the hydrothermal component of the widely used one-dimensional model Water Quality for River-Reservoir Systems (WQRRS) supported by the U.S. Army Corps of Engineers. Comparisons using a Northern California reservoir, Lake Shasta, showed that both models yield similar results with respect to energy budget and temperature profile calculations.

To investigate lake sensitivity to increases or decreases in air temperature, first an approach was developed for generating characteristic deep, intermediate, and shallow hypothetical lakes. The approach was based on the principle of the MIT wind-mixing model.

Regional sensitivity analyses of lake stratification on air temperature change were performed for all latitudes (every 5 degrees). The presence of ice cover and convective overturn (mixing of the water column) were the major indicators used to determine the hydrophysical state of the lakes. The following conclusions can be drawn from the first part of the study in which hypothetical lakes were simulated with the IWEP model using longitudinally averaged meteorological data for a given latitude:

i. The results suggest that the sensitivity of lake stratification to changes in air temperature greatly increases in the transition zones. The two transition zones are: 1) the subtopic zone, where lakes can change from warm monomictic to dimictic (about 30^{o}-45^{o} N/S latitude), and; 2) the subpolar zone, where lakes can change from dimictic to cold monomictic (about 65^{o}-80^{o} N/S latitude).

`ii. Stratification in shallow and intermediate lakes was slightly sensitive to changes in air temperature in subtropical regions. On the other hand, stratification of deep lakes, was significantly sensitive to air temperature changes in this same region. In temperate and polar regions the sensitivity of lake stratification to changes in air temperature was important for all lake depths.

iii. Turnover characteristics of subtopic and subpolar lakes are significantly affected by warmer atmospheric temperatures. In these lakes, turnover was found to begin earlier in the year than under existing conditions. Also the duration of well mixed conditions was longer. On the other hand, cooler atmospheric temperatures led to a delay in the onset of lake turnover and to a reduction in the length of well mixed conditions.

iv. The duration of ice cover is most sensitive to changes in air temperature in subpolar and polar lakes regardless of depth. In subtropical regions ice formation in lakes is less sensitive to atmospheric temperature changes, but it tends to be more sensitive to lake depth. A deep lake is more prone to ice cover formation than a shallow lake.

v. Changes in the duration of overturn periods by as much as 10 days were common for changes of 5 ^{o}C in air temperature. These changes can be important particularly in eutrophic lakes which depend on mixing events to offset negative impacts of stratification, e.g., anoxic conditions in the hypolimnion.

vi. Sensitivity analysis showed that dependency of indicators selected to monitor hydrophysical conditions of the lake is monotonous and continuous. Effect of changing climate is equivalent to corresponding change in geographic location, approximately one latitude degree per one degree Celsius of air temperature.

In the final stage of the study, potential impacts of climate change were assessed for real lakes. The selected lakes are located within the previously identified sensitive regions, e.i., subtropical and subpolar zones. They are treated as prototypes, using simplified assumptions in morphology and hydrologic boundary conditions.

Present conditions were simulated with historical climate data, while future conditions, i.e., a doubling in the concentration of atmospheric CO_2, were simulated with GFDL climate model results. The simulation of existing conditions corresponded well with observed data. The annual distribution of stratification patterns and ice formation agreed with observations reported in the limnological literature. Analysis under conditions of changed climate assumed led to the following conclusions:

i. In the warmer lower latitudes periods of stratification are likely to be enhanced. This case is typical of subtropical zones, where a warm monomictic lake can potentially become oligomictic, as in the case of Lake Geneva and Shasta Lake.

ii. In the colder higher latitudes the frequency of overturn is likely to increase. There is a potential for subpolar lakes to change from cold monomictic to dimictic as in the case of Great Bear Lake.

iii. Ice formation in subpolar regions can be reduced or totally suppressed as in the case of Lake Ladoga.

iv. Of the nine lakes selected for study, four were subject to changes in stratification patterns and duration of ice cover. Even if there was no change in stratification pattern, as in the case of Lake Ladoga, Ezequiel Ramos Reservoir, Lake Maggiore, Changshou-Hu Reservoir, or Lake Biwa-Ko, water temperature can change significantly enough to induce alterations in water quality and lake biota, or changes the local climate as in the case of Lake Ladoga.

Our study provides a first step to the systematic evaluation of the impacts of global climate change on hydrothermal dynamics of lakes. The study incorporates many simplifying assumptions, both about the physical system and the computer modeling. Future research can be pursued in the following areas:

i. Investigation of the effects of additional climatic variables, such as relative humidity or cloud cover, by using GCM predictions (or testing sensitivities).

ii. Use of other GCMs for comparison purpuses and uncertainty assessment.

iii. Use of more realistic representations of lake morphology, lake inflow, and outflow, and in-situ meteorological variables.

iv. Modeling of a comprehensive range of water quality constituents with an appropriate model.

REFERENCES

Bolin, B., B. R. Doos, J. Jager, and R. A. Warrick, 1986. The Greenhouse Effect Climatic Change and Ecosystems: A Synthesis of the Present Knowledge, SCOPE 29, John Wiley, New York.

Deadoff, J. V., 1970. Convective Velocity and Temperature Scales for the Unstable Planetary Boundary Layer. J. Atmosph. Sci., Vol. 27. p. 1211-1213.

Imberger, J., and J. C. Patterson, 1990. Physical Limnology. Advances in Applied Mechanics, Vol. 27.

Fiering, M.B., and N.C. Matalas, 1990. Decision-Making under Uncertainty. Edited by P. E. Waggoner in Climate Change and U.S. Water Resources. John Wiley and Sons, p. 75-84.

Goldman, C. R., and A. J. Horne, 1983. Limnology. McGraw-Hill Book Company.

Harrison S. P., 1990. An Introduction to General Circulation Modelling Experiments with Raised CO_2. IIASA Working Paper, WP-90-27, Laxenburg, Austria.

Henderson-Sellers, B.(1984). Engineering Limnology. Boston, Pitman Advanced Publications Program, Series title: Monographs and Surveys in Water Resources Engineering.

Hondzo M. and H. G. Stefan, 1991. Three Case Studies of Lake Temperature and Stratification Response to Warmer Climate. Water Resources Research, Vol. 27, No. 8, p. 1837-1846, August.

Hydrologic Engineering Center (HEC),1978. Water Quality For River Reservoir Systems (WRRRS).

Imberger, J. and J. C. Patterson, 1990. Physical Limnology. Edited by Hutchinson, J. W. and W. Y. Theodore, in Advances in Applied Mechanics, Vol. 27, p. 303-475.

Intergovernmental Panel on Climate Change (IPCC), 1992. Climate Change 1992: The supplementary Report to the IPCC Scientific Assessment. Edited by J. T. Houghton, B. A. Callander, and S. K. Varney; New York: Cambridge University Press.

Jacoby H. D., 1990. Water Quality. Edited by P. E. Waggoner in Climate Change and U.S. Water Resources. John Wiley and Sons, p. 307-328.

Kaczmarek, Z., and D. Krasuski, 1991. Sensitivity of Water Balance to Climate Change and Variability. IIASA, WP-91-047.

Kalkstein, S. L., 1991. Global Comparisons of Selected GCM Control Runs and Observed Climate Data. Environmental Protection Agency, Policy, Planning and Evaluation (PM-221), 21P-2002, April.

Kundzewicz, Z. W. and Somlyódy, 1993. Climatic Change Impact on Water Resources -- a Systems View. IIASA Working Paper (forthcoming).

Lachavanne, J. B., 1980. Les Manifestations de L'eutrophisation des Eux dans un Grand Lac Profond, Le Lemann (Suisse). Schweiz Z. Hydrol., Vol. 42, No. 2, p. 127-154.

Leemans, R., and W. P. Cramer, 1991. The IIASA Database for Mean Monthly Temperature, Precipitation, and Cloudiness on a Global Scale. IIASA RR-91-18, International Standard Book Number 3-7045-0113-1, 68 pp.

Lettenmaier, D. P., and T. Y. Gan, 1990. Hydrologic Sensitivities of the Sacramento-San Joaquin River Basin, California, to Global Warming. Water Resources Research, Vol. 26, No. 1, p. 69-86.

Manabe, S., Stouffer, R.J., 1980. Sensitivity of a climate model to an increase of CO_2 concentration in the atmosphere. J. Geophys. Res., v. 85(C10), pp. 5529-5554.

Markofsky, M., and D. R. F. Harleman, 1971. A predictive Model for Thermal Stratification and Water Quality in Reservoirs. Ralph M. Parsons Laboratory for Water Resources and Hydrodynamics, Report No. 134, MIT, Civil Engineering, 71-4.

Meyer, G.K., and G. T. Orlob, 1992. Global Climate Change Effects on Water Quality. Saving a Threatened resource - In Search of Solutions. Proceedings, Water Forum '92, ed. Mohamend Karamouz. American Society of Civil Engineers, Baltimore, August.

Mitchell, J. F. B., 1989. The "Greenhouse" Effect and Climate. Reviews of Geophysics, V 27,1, p. 115-139, February.

Müller, M. J., 1982. Selected Climatic Data for a Global Set of Standard Stations for Vegetation Science. Dr. W. Junk Publishers, The Hague, Netherlands.

Nash, L.L. and P. Gleick, 1991. Sensitivity of Streamflow in the Colorado Basin to Climatic Changes. Journal of Hydrology, Vol. 125 N3-4, p. 221-241, July.

Octavio H., K. A., Jirka, G. H., and D. R. F. Harleman, 1977. Vertical Transport Mechanisms in Lakes and Reservoirs. Massachusetts Institute of Technology, Department of Civil Engineering, Report No. 227, August.

Orlob, G. T., 1983. Mathematical Modeling of Water Quality: Streams, Lakes, and Reservoirs. International Series on Applied Systems Analysis, John Wiley and Sons., New York, 509 pp.

Orlob, G. T., G. K. Meyer, J. DeGeorge, and C. L. Christensen, 1990. Impacts of Global Warming on Water Quality in River-Reservoir Systems. Department of Civil Engineering, University of California, Davis. Proceedings of an International Symposium on Global Warming held in Leningrad, USSR, June.

Schwoerbel, J., 1987. Handbook of Limnology. Ellis Horwood Limited, Halsted Press: a division of John Wiley and Sons.

State of California Department of Fish and Game (SCDFG), 1968. Recommendations on Thermal Objectives for Water Quality Control, Policies on the Interstate Waters of California. Water Project No. 7.

Szilágyi F., and L Somlyódy, 1991. Potential Impacts of Climatic Changes on Water Quality in Lakes. XX General Assembly of the IUGG (11-24 August 1991, Vienna).

Telegadas K., and J. London, 1954. A Physical Model of the Northern Hemisphere Troposphere for Winter and Summer. New York University College of Engineering Research Division. Department of Meteorology, February.

Tennessee Valley Authority (TVA), 1972. Heat and Mass Transfer between a water Surface and the Atmosphere. TVA Water Resources Research Engineering Laboratory, Norris, TN report 14, 123 pp.

UK Meteorological Office, 1966. Tables of Temperature, Relative Humidity and Precipitation for the World, Part V, Asia, HMSO, London, UK.

UK Meteorological Office, 1972. Tables of Temperature, Relative Humidity, Precipitation and Sunshine for the World. Part III, Europe and the Azores, HMSO, London, UK.

UK Meteorological Office, 1973. Tables of Temperature, Relative Humidity and Precipitation for the World, Part VI, Australasia and Pacific Ocean, HMSO, London, UK.

UK Meteorological Office, 1978. Tables of Temperature, Relative Humidity and Precipitation for the World, Part II, Central and South America, the West Indies and Bermuda, HMSO, London, UK.

UK Meteorological Office, 1980. Tables of Temperature, Relative Humidity, Precipitation and Sunshine for the World, Part I, North America and Greenland (including Hawaii and Bermuda), HMSO, London, UK.

UK Meteorological Office, 1983. Tables of Temperature, Relative Humidity, Precipitation and Sunshine for the World, Part IV, Africa, the Atlantic Ocean South 35^{O}N and the Indian Ocean, HMSO, London, UK.

United Nations Environment Programme (UNEP), 1987-1990. Data Book of World Lake Environments (A Survey of the State of the World Lakes). International Lake Environment Commitee. Otsu, Japan, Vols. 1-4.

Waggoner, P. E., 1990. Climate Change and the U.S. Water Resources. John Wiley and Sons, New York, 496 pp.

Walter, H. and H. Lieth, 1960-1967. Klimadiagram-Weltatlas, Gustav Fischer Verlag, Stuttgart Germany.

Weather Bureau, 1959. World Weather Records 1941-1950, U.S. Department of Commerce, Washington, D.C., USA.

Wetherald, R. T., and S. Manabe, 1988. Cloud Feedback Processes in a General Circulation Model. J. of Atmospheric Sciences, 45, No.8, p 1397-1415, April.

Wetzel, R. G. 1983. Limnology. Saunders College Publishing, Second Edition.

Wood, E. F., 1991. Land Surface-Atmosphere Interactions for Climate Modeling. Kluwer Academic Publishers, the Netherlands.

Zinoviev, A. T., A. A. Kuzmin, and I. E. Masliev, 1990. Mathematical Modelling of Thermal Stratification of Deep Reservoirs. Application of computers in hydrotechniques and protection of water resources (in Russian). Verna, BAN, p. 346-57.

APPENDIX

A SIMPLIFIED WIND MIXING MODEL FOR LAKES

Let's consider a lake with total depth H, depth of epilimnion h fully mixed with temperature T_E, and a hypolimnion with temperature T_H, as shown in Figure 6.1.

The thermal energy exchange equation for the hypolimnion can be written as:

$$\frac{d}{dt}\left(\int_{0}^{H_t - h} c_H \rho_H T_H A(z)dz\right) = -q_E c_H \rho_H T_H - \phi_0 \qquad (1)$$

Rate of change of heat due to entrainment in hypolimnion	Flux of heat from the hypolimnion	Heat exchange with the lake bed

where:

T_H = hypolimnion temperature, $T_H = T_H(t)$;
A = cross sectional area, $A = A(z)$;
ρ_H = density of the hypolimnion, $\rho_H = \rho_H(t)$;
t = time;
z = vertical coordinate;
H_t = total depth of lake;
h = epilimnion depth;
q_e = flow rate of the hypolimnetic water to the epilimnion due to entrainment:
$q_e = A(H_t - h)\, dh/dt$
ϕ_0 = heat exchange with the lake bed, which will be neglected.

The heat exchange of the epilimnion is:

$$\frac{d}{dt}\left(\int_{H_t - h}^{H_t} c_p \rho_E T_E A(z)dz\right) = \phi_s + q_e c_p \rho_H T_H - \phi_0 \qquad (2)$$

rate of change of heat contents in the epilimnion	surface heat flux	influx of heat from the hypolimnion	Heat exchange with the bottom

where:

T_E = epilimnion temperature, $T_E = T_E(t)$;
ρ_E = density of the epilimnion, $\rho_E = \rho_E(t)$;
ϕ_S = surface heat flux.

The mechanical energy budget equation is

$$\frac{dP}{dt} = k', \tag{3}$$

where P is a modified potential energy, the sum of gravitational and buoyancy forces (Imberger, 1990), and is expressed as

$$\frac{dP}{dt} = \left(\frac{\partial P}{\partial T}\right)_{\phi_s=0} + \left(\frac{\partial P}{\partial t}\right)_{dh/dt=0} \tag{4}$$

Potential energy due to gravity

Potential energy due to buoyancy

and k' is the rate of change of kinetic energy supply:

$$k' = \rho_E u_*^3, \tag{5}$$

where u_* is the shear velocity across the water-air interface (wind-related stress).

In the resulting set of three ordinary differential equations (Equations 1 to 3) the unknown variables are T_E, T_H, h. Integration of Equation (1) neglecting the heat exchange with the lake bed reduces the hypolimnion heat exchange balance to the following:

$$c_p \rho_H V_H (H_t - h) \frac{dT_H}{dt} = 0, \tag{6}$$

where V_H is the volume of the hypolimnion.

Therefore, T_H = constant (with the accuracy of neglected heat exchange with lake bed).

Integration of Equation (2) gives the heat balance equation for the epilimnion:

$$c_p V_E \frac{d}{dt}(T_E \rho_E) + c_p \rho_E T_E \frac{dh}{dt} A(H_t - h) = \phi_s + c_p \rho_H T_H A(H_t - h) \frac{dh}{dt} \tag{7}$$

The gravity part of potential energy is:

$$\left(\frac{\partial P}{\partial t}\right)_{\phi_s=0} = g \int_0^{H_t - h} \rho_H A(z) z dz + g \int_{H_t - h}^{H_t} \rho_E A(z) z dz \tag{8}$$

This expression can be further simplified if we consider that

1) T_H = constant implies that ρ_H is also a constant,

2) a lake morphometry function $z_E(h)$ is defined as:

$$z_E(h) = \frac{1}{V_E}\left[\int_{H-h}^{H} A\,z\,dz - (H-h)\,V_E\right] = \frac{1}{V_E}\int_{0}^{h} t\,A(t-H+h)dt, \qquad (9)$$

3) adiabatic conditions are preserved during mixing, implying we can set $\partial\rho/\partial T = 0$.

Thus, the gravity part of potential energy (Equation 8) becomes:

$$\left(\frac{\partial P}{\partial t}\right)_{\phi_s=0} = z_E(h)(\rho_H - \rho_E)gA(H_t - h)\frac{dh}{dt} \qquad (10)$$

To calculate buoyancy forces, consider an infinitesimal layer at the surface, δh, experiencing a change in density $\delta\rho$. Instantaneous mixing of this layer then changes the epilimnion density to ρ'_E and under these circumstances the infinitesimal potential energy change due to buoyancy can be calculated as

$$\left(-\frac{\delta P}{g}\right)_{\frac{dh}{dt}=0} = \int_{H_t-h}^{H_t-\delta h} \rho_E A z dz + \int_{H-\delta h}^{H_t} (\rho_E + \delta\rho) A z dz - \int_{H_t-h}^{H_t} \rho'_E A z dz \qquad (11)$$

Equation (11) can be simplified on the basis of following assumptions:

1) for a small δh, the area A can be considered constant ($A = A_S$)

2) with $\rho = M / V$, where M is mass and V is volume, the change in density is expressed as:

$$\rho'_E - \rho_E = \delta\rho\frac{\delta h\, A_s}{V_E} \qquad (12)$$

3) changes in temperature due to surface heating can be approximated as

$$\phi_s \delta t A_s = \delta V c_p \rho \delta T \qquad (13)$$

and

$$\delta T = \delta\rho\frac{1}{\left(\frac{d\rho}{dt}\right)}. \qquad (14)$$

After rearrangements the rate of change of potential energy due to buoyant forces can be expressed as:

$$(\delta P)_{\frac{dh}{dt}=0} = -g(h - z_E(h))\, A_s \frac{\phi_s\, \delta t}{c_p\, \rho}\frac{dp}{dT} \qquad (15)$$

Finally, setting the rate of change of kinetic energy equal to the total rate of change of potential energy yields the necessary differential equation for h(t) (cf Equation 5):

$$k' = -g(h - z_E(h))\frac{\phi_s A_s}{c_p \rho_E}\left(\frac{d\rho}{dT}\right)\Big|_{T=T_E} + g(\rho_H - \rho_E)\frac{dh}{dt} z_E(h) A(H_t - h) \qquad (16)$$

Water density (ρ) as a function of water temperature was calculated using the Gephard formula (Henderson-Sellers, 1984)

$$\rho = \rho_o(1 - k_1|T - T_o|k_2) \qquad (17)$$

where:

T_o = reference temperature (= 4.029 ^oC);
ρ_o = reference density (= 999.973 kg/m^3);
K_1 = constant (= 9.207 X 10^{-6});
K_2 = constant (= 1.895).

Numerical solution of the resulting set of ordinary differential equations was obtained using the 4th order Runge-Kutta method.